

# Spectral Densities for Hot QCD Plasmas in a Leading Log Approximation

Juhee Hong and Derek Teaney

*Department of Physics and Astronomy, Stony Brook University,*

*Stony Brook, New York 11794-3800, United States*

(Dated: October 24, 2018)

## Abstract

We compute the spectral densities of  $T^{\mu\nu}$  and  $J^\mu$  in high temperature QCD plasmas at small frequency and momentum,  $\omega, k \sim g^4 T$ . The leading log Boltzmann equation is reformulated as a Fokker Planck equation with non-trivial boundary conditions, and the resulting partial differential equation is solved numerically in momentum space. The spectral densities of the current, shear, sound, and bulk channels exhibit a smooth transition from free streaming quasi-particles to ideal hydrodynamics. This transition is analyzed with conformal and non-conformal second order hydrodynamics, and a second order diffusion equation. We determine all of the second order transport coefficients which characterize the linear response in the hydrodynamic regime.

arXiv:1003.0699v3 [nucl-th] 11 Sep 2010

## I. INTRODUCTION

In relativistic heavy ion collisions a non-abelian plasma is formed which rapidly expands and evolves. There is a growing body of evidence from the Relativistic Heavy Ion Collider (RHIC) that this material equilibrates and can be characterized with viscous hydrodynamics [1, 2]. Indeed, viscous simulations of RHIC events indicate that the shear viscosity to entropy is remarkably small [3–9]

$$\frac{\eta}{s} < 0.4 \hbar, \quad (1.1)$$

and the preferred value is close to the AdS/CFT prediction,  $\eta/s = \hbar/4\pi$  [10, 11]. From a theoretical perspective it is important to corroborate this phenomenological conclusion from first principle lattice QCD simulations. It is also important for lattice simulations to characterize what this nearly perfect fluid is like. For instance, at weak coupling there is a clear distinction between the inverse temperature  $\sim 1/T$  and the typical relaxation time  $\sim 1/g^4 T$  [12, 13], and consequently kinetic theory can be used to describe the real time dynamics of the plasma. In contrast, at least for the strongly coupled gauge theories which can be studied with AdS/CFT, there is no distinction between these time scales, and a quasi-particle description is hopeless [14, 15]. This is reflected by the fact that there is no visible transport peak in strongly coupled spectral densities [16, 17].

Lattice QCD simulations at finite temperature can measure Euclidean correlators of conserved currents,  $\langle J(\tau, \mathbf{x})J(0, \mathbf{0}) \rangle$ . These correlators are related to the spectral density of the corresponding operators by an integral transform [18]

$$\int d^3\mathbf{x} e^{i\mathbf{k}\cdot\mathbf{x}} \langle J(\tau, \mathbf{x})J(0, \mathbf{0}) \rangle = \int \frac{d\omega}{2\pi} \rho^{JJ}(\omega, \mathbf{k}) \frac{\cosh(\omega(\tau - 1/2T))}{\sinh(\omega/2T)}. \quad (1.2)$$

Generally, only the gross features of the spectral density can be determined from Euclidean measurements [19, 20]. Nevertheless, the urgent need for non-perturbative information about transport and other real time processes is evident from the strenuous analysis of available lattice data by several groups [21–26]. In an effort to characterize the response more completely, a number of lattice groups have begun to simulate the current-current correlators at finite spatial momentum [27, 28], which reveals the real time information hidden in the Euclidean data as far as possible. The primary goal of this work is to calculate the spectral densities at finite  $\omega$  and  $\mathbf{k}$  at weak coupling for all possible combinations of  $T^{\mu\nu}$  and  $J^\mu$ . At zero  $\mathbf{k}$  the weakly coupled shear, bulk, and current spectral weights have been determined previously in a full leading order calculation [29, 30]. The spectral weights computed in this work exhibit in detail the transition from free-streaming quasi-particles to hydrodynamics. Ultimately, these perturbative spectral densities can be compared to the AdS/CFT and to the lattice, although a fair comparison to the lattice data requires a model for the high frequency continuum [31].

At weak coupling the kinetics of hot plasmas consists of several processes [12, 32]. First, the streaming of hard particles creates a random soft background field which causes momentum diffusion of the instigating hard particles. Second, there are collisions between the hard particles which cause an  $O(1)$  change in a particle’s direction. Finally, there is collinear bremsstrahlung which plays a particularly important role in the equilibration of the highest momentum modes [33]. In the current work we will reanalyze the Boltzmann equation and make the diffusive process more explicit by reformulating the evolution as a Fokker-Planck equation. This analysis is limited

to a leading log approximation where the hard collisions and collinear bremsstrahlung are neglected for typical particles<sup>1</sup>.

The QCD kinetic theory described above has been used to compute the transport coefficients in high temperature gauge theories [34–36], and to provide an intriguing, but incomplete, picture of equilibration in heavy ion collisions [33, 37–39]. Ultimately, one would like to simulate heavy ion event using the QCD Boltzmann equation, quantifying equilibration in the weakly coupled limit. While there has been considerable progress in understanding the dynamics of the soft background gauge fields out of equilibrium [40–42], there have been only nascent steps in simulating the coupled particle field problem [43, 44]. As a by-product of the spectral weight calculation, we have made some (limited) progress in simulating the QCD kinetic theory. Traditionally, the shear viscosity is determined by minimizing a variational ansatz. However, when computing the spectral weights at finite  $\mathbf{k}$ , the variational ansatz would have to be two dimensional, and would have to capture a complicated structure reflecting the transition from Landau damping to hydrodynamics. In the two dimensional case it is easier to discretize momentum space and to solve the Fokker Planck equation directly. Finding the correct solution requires understanding the appropriate boundary conditions. In particular, there is an absorptive boundary condition at  $\mathbf{p} = 0$  which accounts for the flux of particles from the temperature scale to the Debye scale and rapid number changing processes in the  $\mathbf{p} \rightarrow 0$  limit [36]. Section II reviews this boundary condition and shows how gluon number equilibrates while conserving energy and momentum. Now that the problem of determining spectral densities has been reformulated as a definite initial value problem, the resulting numerical procedure can be used to simulate jet medium interactions in detail. In fact, it was this goal that led to the present work.

Throughout, we will denote 4-vectors with capital letters  $P, Q$  and use  $\mathbf{p}, \mathbf{q}$  for their 3-vector components,  $E_p, E_q$  for their energy components, and  $p, q$  for  $|\mathbf{p}|, |\mathbf{q}|$ . Spatial 4-vectors and 3-vectors follow an analogous convention, *e.g.*  $X, Y$  and  $\mathbf{x}, \mathbf{y}$ , respectively. Our metric convention is  $[-, +, +, +]$ , so that  $u_\mu u^\mu = -1$ . We will notate the Bose and Fermi equilibrium distribution functions with  $n_p^B = 1/(e^{p/T} - 1)$  and  $n_p^F = 1/(e^{p/T} + 1)$ , but will drop the  $B/F$  label when the appropriate statistics are clear from context. Momentum space integrals are abbreviated,  $\int_{\mathbf{p}} \equiv \int d^3p/(2\pi)^3$ .

## II. LINEARIZED BOLTZMANN EQUATION

Our starting point is the Boltzmann equation

$$(\partial_t + v_{\mathbf{p}} \cdot \partial_{\mathbf{x}})f(t, \mathbf{x}, \mathbf{p}) = C[f, \mathbf{p}], \quad (2.1)$$

which we will linearize around the equilibrium distribution with constant temperature  $T_o$

$$f(t, \mathbf{x}, \mathbf{p}) = n_p + \delta f(t, \mathbf{x}, \mathbf{p}), \quad n_p = \frac{1}{e^{p/T_o} - 1}. \quad (2.2)$$

The background is characterized by the energy density  $e_o$ , the pressure  $\mathcal{P}_o$ , a squared sound speed  $c_s^2$ , and the specific heat  $Tc_v$ . Initially we will consider only pure glue theory and subsequently

---

<sup>1</sup> As discussed in the text, this is not exactly true. Bremsstrahlung will determine the boundary conditions of the Fokker Plank operator as  $\mathbf{p} \rightarrow 0$ , but otherwise can be neglected.

extend the analysis to include quarks in Section V. In a leading-log approximation, the only diagram is  $t$ -channel gluon exchange. Appendix A re-interprets the linearized Boltzmann equation (at leading log) as a Fokker-Planck equation, which is useful in subsequent analysis. Appendix A extends the analysis of Refs. [34, 45, 46] to general partial waves, and gives explicit expressions for the leading log gain terms. The gain terms do not affect the shear viscosity, since they only contribute to the  $\ell = 0$  and  $\ell = 1$  partial waves. However, the gain terms do affect the spectral weights at finite  $\mathbf{k}$  and  $\omega$  which is the primary focus of the current work.

Following Appendix A, the linearized Boltzmann equation can be written

$$(\partial_t + v_{\mathbf{p}} \cdot \partial_{\mathbf{x}})\delta f = T\mu_A \frac{\partial}{\partial \mathbf{p}^i} \left( n_p(1+n_p) \frac{\partial}{\partial \mathbf{p}^i} \left[ \frac{\delta f}{n_p(1+n_p)} \right] \right) + \text{gain terms}, \quad (2.3)$$

where  $\mu_A$  is the drag coefficient of a high momentum gluon in the leading log approximation scheme [47, 48]

$$\frac{d\mathbf{p}}{dt} = -\mu_A \hat{\mathbf{p}}, \quad \mu_A \equiv \frac{g^2 C_A m_D^2}{8\pi} \log \left( \frac{T}{m_D} \right), \quad (2.4)$$

and the Debye mass for a pure glue theory is<sup>2</sup>

$$m_D^2 = \frac{g^2 C_A}{d_A} \nu_g \int_{\mathbf{p}} \frac{n_p(1+n_p)}{T} = \frac{g^2 T^2}{3} N_c. \quad (2.5)$$

Without the gain terms, Eq. (2.3) is a Fokker-Planck equation describing a random walk of the hard particles.

In the diffusion process, the momentum-space current is given by

$$\mathbf{j}_p = -T\mu_A n_p(1+n_p) \frac{\partial}{\partial \mathbf{p}} \left[ \frac{\delta f}{n_p(1+n_p)} \right], \quad (2.6)$$

and the work on the particles per time, per Degree Of Freedom (DOF), per volume can be found by multiplying both sides of Eq. (2.3) by  $E_{\mathbf{p}}$  and integrating over phase space

$$\frac{dE}{dt} \equiv \int \frac{d^3\mathbf{p}}{(2\pi)^3} \hat{\mathbf{p}} \cdot \mathbf{j}_p. \quad (2.7)$$

The momentum transfer (per time, per DOF, per volume) is similarly

$$\frac{d\mathbf{P}}{dt} \equiv \int \frac{d^3\mathbf{p}}{(2\pi)^3} \mathbf{j}_p. \quad (2.8)$$

With these definitions and Appendix A, the gain terms are

$$\text{gain terms} = \frac{1}{\xi_B} \left[ \frac{1}{p^2} \frac{\partial}{\partial p} p^2 n_p(1+n_p) \right] \frac{dE}{dt} + \frac{1}{\xi_B} \left[ \frac{\partial}{\partial \mathbf{p}} n_p(1+n_p) \right] \cdot \frac{d\mathbf{P}}{dt}, \quad (2.9)$$

---

<sup>2</sup> We follow an almost standard notation. The dimensions of the adjoint and fundamental representations are  $d_A = N_c^2 - 1$  and  $d_F = N_c$ . The Casimirs of the adjoint and fundamental are  $C_A = N_c$  and  $C_F = (N_c^2 - 1)/2N_c$ . The trace normalization of the adjoint and fundamental are  $T_A = N_c$  and  $T_F = 1/2$ .  $\nu_g = 2d_A$  and  $\nu_q = 2d_F$  count the spin and color degrees of freedom for gluons and quarks respectively.

where for subsequent use we have defined

$$\xi_B \equiv \int \frac{d^3\mathbf{p}}{(2\pi)^3} n_p(1+n_p) = \frac{T^3}{6}, \quad \xi_F \equiv \int \frac{d^3\mathbf{p}}{(2\pi)^3} n_p(1-n_p) = \frac{T^3}{12}. \quad (2.10)$$

In this form it is straightforward to verify that energy and momentum are conserved during the forward evolution of the linearized Boltzmann equation described by Eq. (2.3) and Eq. (2.9). What is less obvious is that gluon number is not conserved, as will be discussed in the next section.

### A. Boundary conditions and particle flux to low momentum

The resulting integral differential equation is ill-posed without boundary conditions. We will discuss the boundary conditions at low and high momentum respectively.

#### 1. Boundary conditions at zero momentum and number non-conservation

To discuss the appropriate boundary conditions for the gluon number, consider the excess of soft gluons within a small ball of radius  $\Delta p \sim gT$  centered at  $\mathbf{p} = 0$

$$\int_{p=0}^{p=\Delta p} \frac{d^3\mathbf{p}}{(2\pi)^3} n_p(1+n_p)\chi(\mathbf{p}) \simeq \frac{T^2}{2\pi^2}\chi(\mathbf{0})\Delta p, \quad (2.11)$$

where here and below we define

$$\delta f(\mathbf{p}) \equiv n_p(1+n_p)\chi(\mathbf{p}). \quad (2.12)$$

Since it is easy to emit a soft gluon it is easy to intuit that the appropriate boundary condition is

$$\chi(\mathbf{p})|_{\mathbf{p} \rightarrow 0} = 0. \quad (2.13)$$

As discussed in the introduction, Bremsstrahlung can be neglected for momenta of order  $\sim T$  in a leading log approximation. However, since the Bremsstrahlung rate increases as the momentum is lowered, there is a momentum of order  $\sim gT$  where inelastic processes are important for any arbitrarily small coupling constant. Ref. [36] (see section E) estimates that the total rate for the hard particles to absorb (or emit) a gluon from the ball of radius  $\Delta p \sim gT$  is

$$\Gamma_{1 \leftrightarrow 2}^{\text{total}} \sim g^4 T \int_0^{\Delta p} \frac{dp}{p} f(p) \sim g^4 T^2 \int_0^{\Delta p} \frac{dp}{p^2}. \quad (2.14)$$

The infrared divergence of the integral is cut off by the thermal mass of the radiated gluon  $m \sim gT$ , so that the total rate is of order  $g^3 T$

$$\Gamma_{1 \leftrightarrow 2}^{\text{total}} \sim \frac{g^4 T^2}{m} \sim g^3 T. \quad (2.15)$$

We are interested in the evolution of the system on a time scale,  $1/g^4 T \log(1/g)$ , which is large compared to the inverse radiation rate,  $1/g^3 T$ . As we observe the evolution on this longer time scale, the soft Bremsstrahlung rate will rapidly maintain the equilibrium phase space distribution of soft  $\sim gT$  gluons up to corrections of order of the ratio of these two time scales,  $\sim g$ . Thus, the excess

from equilibrium at small momentum,  $\chi(\Delta p)\Delta p$ , is small at small momentum,  $\chi(gT) = O(g)$ . The boundary condition in Eq. (2.13) is the leading result in the weak coupling limit  $g \rightarrow 0$ . Even in a full leading order analysis (where thermal masses are neglected on external lines), the boundary condition must still be adopted to avoid a divergent soft Bremsstrahlung rate [36]. A consequence of this boundary condition is that gluon number is not conserved during the Fokker Planck evolution as will be discussed in Section II B.

## 2. Boundary conditions at high momentum

At high momentum, the second order differential equation typically consists of an exponentially growing solution and an additional solution behaving at most as a polynomial. Clearly we should select the second solution as physically acceptable.

To determine how to select the appropriate boundary conditions at high momentum, we reexamine the Fokker Planck equation

$$(\partial_t + \mathbf{v}_p \cdot \partial_{\mathbf{x}})\delta f(t, \mathbf{x}, \mathbf{p}) = -\mu_A(1 + 2n_p)\hat{\mathbf{p}} \cdot \frac{\partial \delta f}{\partial \mathbf{p}} + T\mu_A \nabla_{\mathbf{p}}^2 \delta f. \quad (2.16)$$

The motion of the particle excess can be described alternatively by Langevin evolution with drag and random kicks  $\xi(t)$

$$\frac{dp^i}{dt} = -\mu_A(1 + 2n_p)\hat{p}^i + \xi^i(t), \quad \langle \xi^i(t)\xi^j(t') \rangle = 2T\mu_A \delta^{ij} \delta(t - t'). \quad (2.17)$$

At high momentum, we neglect the noise term  $\nabla_{\mathbf{p}}^2 \delta f$ , set  $(1 + 2n_p) \simeq 1$ , and keep only the drag term, yielding

$$(\partial_t + \mathbf{v}_p \cdot \partial_{\mathbf{x}})\delta f(t, \mathbf{x}, \mathbf{p}) = -\mu_A \hat{\mathbf{p}} \cdot \frac{\partial \delta f}{\partial \mathbf{p}}. \quad (2.18)$$

The resulting differential equation is now first order in derivatives and can be used to choose a boundary condition. Specifically we will discretize the first derivative

$$\hat{\mathbf{p}} \cdot \frac{\partial \delta f(t, \mathbf{x}, \mathbf{p})}{\partial \mathbf{p}} = \frac{1}{p_n^2} \left[ \frac{p_{n+1}^2 \delta f(t, \mathbf{x}, p_{n+1}, \theta_{\mathbf{p}}, \phi_{\mathbf{p}}) - p_n^2 \delta f(t, \mathbf{x}, p_n, \theta_{\mathbf{p}}, \phi_{\mathbf{p}})}{\Delta p} \right] \quad (2.19)$$

and use Eq. (2.18) to solve for the first point off the momentum space grid,  $f(t, \mathbf{x}, p_{n+1}, \theta_{\mathbf{p}}, \phi_{\mathbf{p}})$ . This selects the appropriate non-exponentially growing solution.

## B. Evolution of simple initial conditions and the flux of gluons

If  $\delta f(t, \mathbf{x}, \mathbf{p})$  is given some initial condition, the resulting Fokker-Planck evolution will equilibrate, and  $\delta f(t, \mathbf{x}, \mathbf{p})$  will ultimately reach a form described by linearized hydrodynamics. Specifically, the system will be described by a temperature excess  $\delta T(t, \mathbf{x})$  and flow velocity  $U^\mu = (1, u^i(t, \mathbf{x}))$  that obey the equations of linearized hydrodynamics. The distribution function will approach

$$f_{\text{eq}}(t, \mathbf{x}, \mathbf{p}) = \frac{1}{e^{-P \cdot U(t, \mathbf{x}) / (T_o + \delta T(t, \mathbf{x}))} - 1} = n_p + n_p(1 + n_p) \left( p \frac{\delta T(t, \mathbf{x})}{T_o^2} + \frac{p_i}{T_o} u^i(t, \mathbf{x}) \right), \quad (2.20)$$

*i.e.*  $\chi(t, \mathbf{x}, \mathbf{p})$  will approach an equilibrium value

$$\chi_{\text{equil}}(t, \mathbf{x}, \mathbf{p}) = p \frac{\delta T(t, \mathbf{x})}{T_o^2} + \frac{p_i}{T_o} u^i(t, \mathbf{x}). \quad (2.21)$$

It is instructive to examine how the total number of gluons,  $\delta N_{FP} = \int_{\mathbf{p}} \delta f(\mathbf{p})$ , equilibrates during the Fokker-Planck evolution. Integrating both sides of Eq. (2.3) yields two terms

$$\partial_t \delta N_{FP} = \lim_{p \rightarrow 0} \frac{1}{(2\pi)^3} \int p^2 d\Omega_{\mathbf{p}} \cdot \mathbf{j}_{\mathbf{p}} \quad + \quad \frac{-T^2}{2\pi^2 \xi_B} \frac{dE}{dt}, \quad (2.22)$$

where  $\Omega_{\mathbf{p}}$  is an outward directed solid angle. The first term represents a diffusion flux of gluons with momenta of order  $p \sim T$  to momenta of order  $p \sim gT$ . The second term is the number of gluons disturbed from equilibrium per unit time by the random walk of the excess,  $\delta f$ . In a given time step, this number disturbed is proportional to minus the work done on the excess by the bath, *i.e.*  $-dE/dt$  is the work done on the bath by the excess. In general, these two rates are different and number changes accordingly. In equilibrium, however, the two rates are equal and the excess number of gluons remains constant. Specifically, substituting the equilibrium distribution Eq. (2.21), we find a net loss of excess gluons to the Debye scale, and a net gain of excess gluons due to the work on the bath

$$\lim_{p \rightarrow 0} \frac{1}{(2\pi)^3} \int p^2 d\Omega_{\mathbf{p}} \cdot \mathbf{j}_{\mathbf{p}} = -\frac{T\mu_A}{2\pi^2} \delta T, \quad \frac{-T^2}{2\pi^2 \xi_B} \frac{dE}{dt} = +\frac{T\mu_A}{2\pi^2} \delta T. \quad (2.23)$$

Further information about the flux of particles from the temperature to the Debye scale is obtained by analyzing the small momentum limit of Eq. (2.3). (For simplicity, we will ignore any spatial dependence of  $\delta f$ .) The expansion of  $\chi(\mathbf{p})$  near  $\mathbf{p} \simeq 0$  is characterized by its  $\ell = 0$  and  $\ell = 1$  spherical harmonic components

$$\chi(\mathbf{p}) = \left. \frac{d\chi_0(t)}{dp} \right|_{p=0} p + \left. \frac{d\chi_1(t)}{dp} \right|_{p=0} \cdot \mathbf{p}, \quad (2.24)$$

where  $\chi_1$  is the Cartesian translation of  $\chi_{1m}(p)$  in a spherical harmonic expansion. Substituting this form into Eq. (2.3), we notice a divergent rate as  $\mathbf{p} \rightarrow 0$

$$\partial_t \chi(t, \mathbf{p}) = -\frac{2T\hat{\mathbf{p}}}{p} \cdot \left( \mu_A \left. \frac{d\chi_1(t)}{dp} \right|_{p=0} + \frac{1}{T\xi_B} \frac{d\mathbf{P}}{dt} \right). \quad (2.25)$$

Because of this divergent rate, the slope at the origin will rapidly adjust itself to maintain the balance condition

$$\left. \frac{d\chi_1(t)}{dp} \right|_{p=0} = \frac{-1}{T\mu_A \xi_B} \frac{d\mathbf{P}}{dt}. \quad (2.26)$$

Thus the angular dependence of the flux (*i.e.*  $p^2 \mathbf{j}_{\mathbf{p}}$  as  $\mathbf{p} \rightarrow 0$ ) is determined by the momentum transfer to the hard particles by the bath. It is straightforward to verify that the equilibrium solution Eq. (2.21) satisfies this balance condition.

Clearly the evolution of the excess is complicated, and the structure of Eq. (2.3) is quite singular in the infrared. To gain some intuition about the solutions to this equation, we will show how an initial out of equilibrium distribution approaches equilibrium. For simplicity, we will consider two

out of equilibrium initial conditions. The first is spherically symmetric and independent of spatial coordinates, while the second initial condition is also spatially independent but is proportional to the  $\ell = 1$  spherical harmonic. Specifically, for the two cases we have

$$\chi(t, \mathbf{p}) = \chi_{00}(p, t) H_{00}(\hat{\mathbf{p}}) \quad (\text{case 1}) , \quad (2.27)$$

$$\chi(t, \mathbf{p}) = \chi_{10}(p, t) H_{10}(\hat{\mathbf{p}}) \quad (\text{case 2}) , \quad (2.28)$$

where  $H_{00}(\hat{\mathbf{p}})$  and  $H_{10}(\hat{\mathbf{p}})$  are the  $\ell = 0$  and  $\ell = 1$  spherical harmonics. For the initial condition at time  $t_0 = 0$ , we take

$$\left[ p^2 n_p (1 + n_p) \chi_{00}(p, t_0) \quad \text{or} \quad p^2 n_p (1 + n_p) \chi_{10}(p, t_0) \right] \propto \sum_{s=\pm} s e^{-(p-sp_0)^2/2\sigma^2} , \quad (2.29)$$

with  $p_0 = 3T_o$  and  $\sigma^2 = T_o$ . The numerical procedure to solve Eq. (2.3) for the  $\ell = 0$  and  $\ell = 1$  partial waves is elaborated in detail in Appendix B. Briefly, Eq. (2.3) (without the gain terms) is a parabolic differential equation. The momentum space is discretized, an implicit scheme is used to perform the update step, and the conjugate gradient algorithm is used to perform the matrix inversion. Fig. 1(a) and (b) show how the two initial conditions evolve as a function of time. At late times, the two initial conditions approach the equilibrium distribution Eq. (2.21) where the parameters  $\delta T$  and  $u^i$  are determined by the total energy and momentum in the initial state, *e.g.*

$$\mathbf{u} = \frac{\nu_g}{e_o + \mathcal{P}_o} \int \frac{d^3 \mathbf{p}}{(2\pi)^3} \mathbf{p} n_p (1 + n_p) \chi(\mathbf{p}, t_0) . \quad (2.30)$$

We have verified that Eq. (2.22) and Eq. (2.26) are satisfied during the evolution. Although the structure of the evolution equations is quite singular in the infrared, due to the boundary conditions (Eq. (2.13)) and the momentum balance condition (Eq. (2.26)), the final solutions are smooth and generally regular functions of momentum.

### III. SPECTRAL DENSITIES OF $T^{\mu\nu}$

#### A. Preliminaries

Our goal is to compute all spectral functions of  $T^{\mu\nu}$  as a function of  $\omega$  and  $\mathbf{k}$ . To this end, we will compute the retarded Green functions

$$G_R^{\mu\nu\alpha\beta}(\omega, \mathbf{k}) = -i \int_{-\infty}^{\infty} dt \int_{-\infty}^{\infty} d\mathbf{x} e^{+i\omega t - i\mathbf{k}\cdot\mathbf{x}} \theta(t) \left\langle \left[ T^{\mu\nu}(t, \mathbf{x}), T^{\alpha\beta}(0, \mathbf{0}) \right] \right\rangle' , \quad (3.1)$$

and the associated spectral functions

$$\rho^{\mu\nu\alpha\beta}(\omega, \mathbf{k}) = -2 \text{Im} G_R^{\mu\nu\alpha\beta}(\omega, \mathbf{k}) . \quad (3.2)$$

Here the  $'$  indicates that the average is over the partition function in flat space [49]. The distinction is necessary since the easiest procedure to calculate such correlators in kinetic theory is to disturb the theory with a weak external gravitational field.

In the presence of a weak gravitational field, the stress tensor of the fluid in perfect equilibrium is

$$T_{\text{eq}}^{\mu\nu}(X) \equiv (e(T) + \mathcal{P}(T)) u^\mu(X) u^\nu(X) + \mathcal{P}(T) g^{\mu\nu}(X) , \quad (3.3)$$



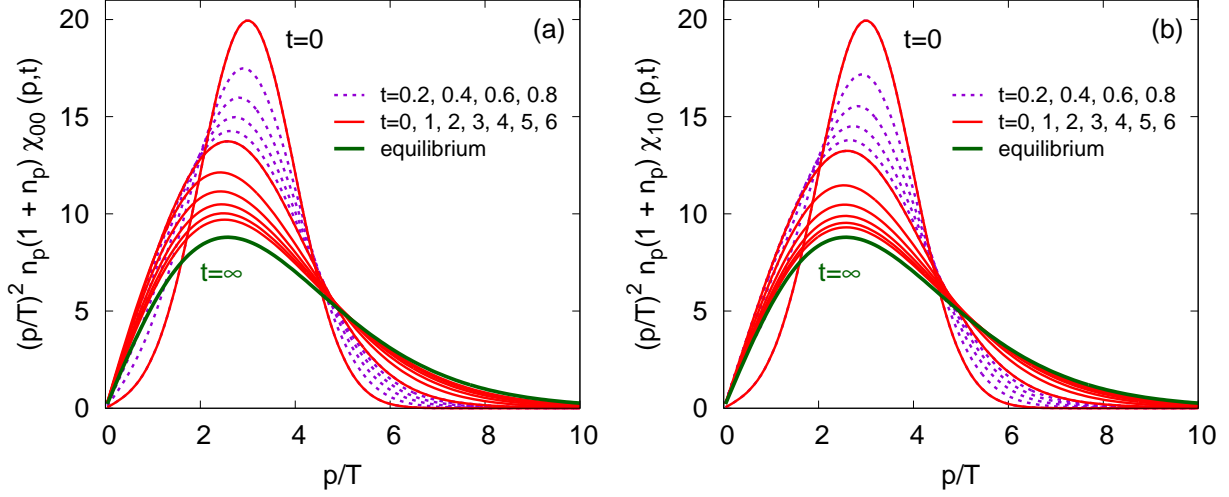


FIG. 1: Evolution of an initial condition towards equilibrium in the linearized Boltzmann equation. (a) A spherically symmetric ( $\ell = 0$ ) initial condition approaching equilibrium at various time steps. Steps are in units of  $T/\mu_A$  with  $\mu_A = g^2 C_A m_D^2 \log(T/m_D)/8\pi$ . (b) An initial condition proportional to the first spherical harmonic  $H_{10}(\hat{\mathbf{p}})$  evolving towards equilibrium. In each plot the dotted lines show time steps of  $0.2T/\mu_A$ . The solid lines show times steps in units of  $1.0T/\mu_A$ .

where  $u^\mu = (1/\sqrt{-g_{00}(X)}, 0)$ . Corrections to this equilibrium form can be found from the modifications to the density matrix which is perturbed by the gravitational field. To linear order in the gravitational field, the action describing material in curved space time is

$$S(g_{\mu\nu}) \simeq S_o + \frac{1}{2} \int d^4X T^{\mu\nu}(X) h_{\mu\nu}(X), \quad (3.4)$$

and the interaction Hamiltonian is

$$H_{\text{int}}(t) = - \int d^3\mathbf{x} \mathcal{L}_{\text{int}} = -\frac{1}{2} \int d^3\mathbf{x} T^{\alpha\beta}(X) h_{\alpha\beta}(X). \quad (3.5)$$

Then following the usual discussion of linear response, we have

$$\langle T^{\mu\nu}(X) \rangle_{h_{\alpha\beta}} = T_{\text{eq}}^{\mu\nu}(X) - \frac{-i}{2} \int d^4Y \theta(X^0 - Y^0) \left\langle [T^{\mu\nu}(X), T^{\alpha\beta}(Y)] \right\rangle' h_{\alpha\beta}(Y). \quad (3.6)$$

In Fourier space we have for  $K = (\omega, \mathbf{k}) \neq 0$ ,

$$\langle T^{\mu\nu}(\omega, \mathbf{k}) \rangle_{h_{\alpha\beta}} = \left. \frac{\partial T_{\text{eq}}^{\mu\nu}}{\partial h_{\alpha\beta}} \right|_{h=0} h_{\alpha\beta}(\omega, \mathbf{k}) - \frac{1}{2} G_R^{\mu\nu\alpha\beta}(\omega, \mathbf{k}) h_{\alpha\beta}(\omega, \mathbf{k}). \quad (3.7)$$

Thus to determine the spectral functions, we will turn on a weak gravitational field in the kinetic theory and determine the attending change in the distribution function and the stress tensor.

To classify the relevant correlators, we will choose  $\mathbf{k}$  along the  $z$  axis. Then the correlators can be classified according to their transformation properties under rotations around the  $z$  axis. In the next sections we will compute the following complete set of response functions:

1.  $G_R^{zxzx}(\omega, k)$  – Shear mode

2.  $G_R^{zzzz}(\omega, k)$  – Sound mode
3.  $G_R^{xyxy}(\omega, k)$  – Tensor mode
4.  $\eta_{\mu\nu}\eta_{\alpha\beta}G_R^{\mu\nu\alpha\beta}(\omega, k)$  – Bulk mode

## B. Shear mode

In this section we will compute the retarded correlator  $G_R^{zzxx}(\omega, k)$  by turning on a gravitational field  $h_{zx}(t, z)$ . Then we will analyze this correlator in the free-streaming and hydrodynamic approximations to determine the high and low frequency limits respectively. The procedure (which is reasonably standard [14, 49, 50]) will be described in detail in this section, and the same procedure will be used subsequently without explanation.

In the presence of a gravitational field, the streaming term of the Boltzmann equation becomes [51, 52]

$$\frac{1}{E_{\mathbf{p}}} \left( P^\mu \frac{\partial}{\partial X^\mu} - \Gamma_{\mu\nu}^\lambda P^\mu P^\nu \frac{\partial}{\partial P^\lambda} \right) f(t, \mathbf{x}, \mathbf{p}) = C[f, \mathbf{p}], \quad (3.8)$$

where

$$\Gamma_{\mu\nu}^\lambda = \frac{1}{2} g^{\lambda\rho} (\partial_\nu g_{\rho\nu} + \partial_\nu g_{\mu\rho} - \partial_\rho g_{\mu\nu}). \quad (3.9)$$

In this equation  $\partial f / \partial P^0$  should be understood as zero. Except in the bulk channel, all temporal components of the metric perturbation are zero

$$g_{ij} \simeq \eta_{ij} + h_{ij}. \quad (3.10)$$

Then we linearize the Boltzmann equation around the equilibrium distribution, which also depends on the background metric

$$f(t, \mathbf{x}, \mathbf{p}) = n_p^h + \delta f(t, \mathbf{x}, \mathbf{p}), \quad n_p^h = \frac{1}{\exp(\sqrt{\mathbf{p}^i(\eta_{ij} + h_{ij})\mathbf{p}^j}/T) \mp 1}. \quad (3.11)$$

Substituting Eq. (3.11) into Eq. (3.8) and linearizing with respect to  $\delta f$  and  $h_{ij}$  leads to the following equation for  $\delta f$

$$(\partial_t + v_{\mathbf{p}} \cdot \partial_{\mathbf{x}}) \delta f + n_p(1 + n_p) \frac{p^i p^j}{2E_{\mathbf{p}} T} \partial_t h_{ij} = C[\delta f, \mathbf{p}]. \quad (3.12)$$

In Fourier space, this equation reads

$$(-i\omega + iv_{\mathbf{p}} \cdot \mathbf{k}) \delta f(\omega, \mathbf{k}, p) - i\omega n_p(1 + n_p) \frac{p^i p^j}{2E_{\mathbf{p}} T} h_{ij}(\omega, \mathbf{k}) = T\mu_A \frac{\partial}{\partial p^i} \left( n_p(1 + n_p) \frac{\partial \chi(\mathbf{p})}{\partial p^i} \right) + \text{gain terms}. \quad (3.13)$$

Without the gain terms, this is a linear elliptic partial differential equation which results from the steady state limit parabolic differential equation, as is usually the case. Traditionally, such differential equations are solved by matrix inversion, e.g. by the conjugate gradient method. We

will adopt this approach; in Appendix B, we introduce a spherical harmonic basis and discretize the radial momenta. Then the Fokker-Planck operator is realized with a straightforward second order difference scheme. This procedure, with only  $h_{zx} \neq 0$  for the shear channel, determines  $\delta f(\omega, k)/h_{zx}(\omega, k)$  which can be used in subsequent analysis.

After solving for  $\delta f(\omega, k)$ , the energy-momentum tensor can be computed from kinetic theory

$$T^{zx} = \nu_g \int \frac{d^3 \mathbf{p} \sqrt{-g}}{(2\pi)^3} \frac{p^z p^x}{E_{\mathbf{p}}} \left( n_p^h + \delta f(\omega, k) \right), \quad (3.14)$$

$$= -\mathcal{P}_o h_{zx}(\omega, k) + \left[ \nu_g \int \frac{d^3 \mathbf{p}}{(2\pi)^3} \frac{p^z p^x}{E_{\mathbf{p}}} \frac{\delta f(\omega, k)}{h_{zx}(\omega, k)} \right] h_{zx}(\omega, k). \quad (3.15)$$

Comparison with Eq. (3.7) shows that the term in square brackets is minus the retarded correlator,  $-G^{zxzx}(\omega, k)$ . Fig. 2(a) shows the associated spectral density in the shear channel, and this correlator will be analyzed at low and high frequency in the remainder of this section.

At low frequencies, hydrodynamics in an external gravitational field describes the behavior of this correlator. Hydrodynamics consists of the conservation laws together with a constituent relation

$$\nabla_{\mu} T^{\mu\nu} = 0, \quad T^{\mu\nu} = T_{\text{ideal}}^{\mu\nu} + \pi^{\mu\nu} + \Pi \Delta^{\mu\nu}, \quad (3.16)$$

where  $T_{\text{ideal}}^{\mu\nu} = (e(T) + \mathcal{P}(T))u^{\mu}u^{\nu} + \mathcal{P}(T)g^{\mu\nu}$ ,  $\Delta^{\mu\nu} = g^{\mu\nu} + u^{\mu}u^{\nu}$  is the projector, and  $\pi^{\mu\nu}$  is traceless. The strains  $\pi^{\mu\nu}$  and  $\Pi$  are expanded in gradients,  $\pi^{\mu\nu} = \pi_1^{\mu\nu} + \pi_2^{\mu\nu} + \dots$  and  $\Pi = \Pi_1 + \Pi_2 + \dots$ , with

$$\pi_1^{\mu\nu} = -\eta \sigma^{\mu\nu}, \quad \Pi_1 = -\zeta \nabla_{\gamma} u^{\gamma}. \quad (3.17)$$

Here  $\nabla_{\mu}$  denotes the covariant derivative, the brackets denote the symmetric, traceless, and spatial component of the bracketed tensor

$$\langle A_{\mu\nu} \rangle = \frac{1}{2} \Delta^{\mu\alpha} \Delta^{\nu\beta} \left( A_{\alpha\beta} + A_{\beta\alpha} - \frac{2}{3} g_{\alpha\beta} A_{\gamma}^{\gamma} \right), \quad (3.18)$$

and  $\sigma^{\mu\nu} \equiv 2 \langle \nabla^{\mu} u^{\nu} \rangle$ . The second order theory which describes  $\pi_2^{\mu\nu}$  and  $\Pi_2$  will be discussed in Section IV. The weak gravitational field disturbs the energy momentum tensor away from equilibrium

$$e(t, \mathbf{x}) \simeq e_o + \epsilon(t, z), \quad u^{\mu} \simeq (1, u^i(t, z)), \quad (3.19)$$

where  $\epsilon$  and  $u^i$  are first order in the perturbation. To first order in the field and disturbance the constituent relation becomes

$$T^{ij} = \mathcal{P}_o (\delta^{ij} - h_{ij}) + c_s^2 \epsilon \delta^{ij} - 2\eta \langle \partial^i u^j \rangle - \zeta \delta^{ij} \partial_t u^l - \eta \partial_t \langle h_{ij} \rangle - \frac{3}{2} \zeta \delta^{ij} \partial_t h, \quad (3.20)$$

where  $h = h_{ll}/3$ . The linearized equations of motion are

$$\partial_t \epsilon + (e_o + \mathcal{P}_o) \partial_i u^i = -\frac{3}{2} (e_o + \mathcal{P}_o) \partial_t h, \quad (3.21)$$

$$(e_o + \mathcal{P}_o) \partial_t u^i + \partial_j T^{ji} = -\mathcal{P}_o \partial_j h_{ji}. \quad (3.22)$$

For the shear channel we specialize perturbation given above, with only  $h_{zx}(t, z)$  non-zero. Then the equations of motion are easily solved in Fourier space

$$\epsilon(\omega, k) = 0, \quad u^z(\omega, k) = 0, \quad (e_o + \mathcal{P}_o)u^x(\omega, k) = \frac{\omega k \eta}{-i\omega + \frac{\eta k^2}{e_o + \mathcal{P}_o}}. \quad (3.23)$$

Substituting these results into stress tensor Eq. (3.20), we determine the retarded Green function in a first order hydrodynamic approximation

$$T^{zx}(\omega, k) = -\mathcal{P}_o h_{zx}(\omega, k) - G_R^{zxzx}(\omega, k) h_{zx}(\omega, k), \quad G_R^{zxzx}(\omega, k) = \frac{-\eta \omega^2}{-i\omega + \frac{\eta k^2}{e_o + \mathcal{P}_o}}. \quad (3.24)$$

The imaginary part of this retarded Green function  $G_R^{zxzx}(\omega, k)$

$$\frac{\rho^{zxzx}(\omega, k)}{2\omega} = \frac{\omega^2 \eta}{\omega^2 + \left(\frac{\eta k^2}{e_o + \mathcal{P}_o}\right)^2} \quad (\omega \text{ and } k \text{ small}), \quad (3.25)$$

describes the rapid behavior at small  $k$  and small  $\omega$  seen in Fig. 2(a).

For high frequency, the free streaming Boltzmann equation,

$$(\partial_t + v_{\mathbf{p}} \cdot \partial_{\mathbf{x}}) \delta f + n_p(1 + n_p) \frac{p^i p^j}{2E_{\mathbf{p}}} \partial_t h_{ij} = 0, \quad (3.26)$$

determines the spectral function. Again specializing the discussion to the shear mode where only  $h_{zx}(\omega, k) \neq 0$ , we solve for  $\delta f(\omega, k)$ . Then the stress tensor is

$$T^{zx} = -\mathcal{P}_o h_{zx}(\omega, k) + \left[ \nu_g \int_{\mathbf{p}} \frac{p^z p^x}{E_{\mathbf{p}}} \frac{\delta f(\omega, k)}{h_{zx}(\omega, k)} \right] h_{zx}(\omega, k), \quad \delta f(\omega, k) = \frac{p^z p^x}{E_{\mathbf{p}}} \frac{-\omega h_{zx} n_p (1 + n_p)}{\omega - v_{\mathbf{p}} \cdot \mathbf{k} + i\epsilon}. \quad (3.27)$$

Again the quantity in square brackets is the free streaming prediction for the response function  $-G_R^{zxzx}(\omega, k)$ , and we have introduced the  $+i\epsilon$  in order to specify the retarded response. Taking the imaginary part of the response function (using  $\text{Im} [1/(x + i\epsilon)] = -\pi\delta(x)$ ), we determine the spectral density from the free theory

$$\frac{\rho^{zxzx}(\omega, \mathbf{k})}{2\omega} = \frac{\nu_g \pi^3 \omega^2}{30 k^3} \left(1 - \frac{\omega^2}{k^2}\right) \theta(k - \omega), \quad (\omega \text{ and } k \text{ large}). \quad (3.28)$$

The free solution is shown as a dashed line in Fig. 2(a) and agrees with the full result at large  $\omega$  and  $k$  except near the light cone.

### C. Sound mode

In the sound channel, the only non-zero metric perturbation is  $h_{zz}(\omega, k)$ . The hydrodynamic prediction for  $K \neq 0$  is

$$T^{zz}(\omega, k) = -\mathcal{P}_o h_{zz}(\omega, k) - \frac{1}{2} G^{zzzz}(\omega, k) h_{zz}(\omega, k), \quad G^{zzzz}(\omega, k) = (e_o + \mathcal{P}_o) \frac{c_s^2 \omega^2 - i\Gamma_s \omega^3}{\omega^2 - c_s^2 k^2 + i\Gamma_s k^2 \omega}, \quad (3.29)$$

where  $\Gamma_s = (\frac{4}{3}\eta + \zeta)/(e_o + \mathcal{P}_o)$ . The free prediction is

$$\frac{\rho^{zzzz}(\omega, k)}{2\omega} = \frac{\nu_g \pi^3}{15} \frac{1}{k} \left(\frac{\omega}{k}\right)^4 \theta(k - \omega), \quad (3.30)$$

and is shown in Fig. 2(b).

#### D. Tensor mode

In the tensor channel, the only non-zero metric perturbation is  $h_{xy}(\omega, k)$ . The hydrodynamic prediction is then

$$T^{xy}(\omega, k) = -\mathcal{P}_o h_{xy}(\omega, k) - G_R^{xyxy}(\omega, k) h_{xy}(\omega, k), \quad G_R^{xyxy}(\omega, k) = -i\omega\eta, \quad (3.31)$$

while the free prediction is

$$\frac{\rho^{xyxy}(\omega, k)}{2\omega} = \frac{\nu g \pi^3}{120} \frac{1}{k} \left[ 1 - \left( \frac{\omega}{k} \right)^2 \right]^2 \theta(k - \omega). \quad (3.32)$$

#### E. Bulk mode

To calculate the bulk spectral weight, considerably more care is required. In this case, the system is perturbed by a metric tensor of the following form

$$g_{\mu\nu}(X) = (1 + H(X))\eta_{\mu\nu}. \quad (3.33)$$

If the gravitational perturbation is independent of time, hydrostatic equilibrium will be reached when  $T(\mathbf{x})\sqrt{-g_{00}(\mathbf{x})}$  reaches a constant. Motivated by this observation, we show that for a conformally invariant theory, the distribution

$$n_p^H(t, \mathbf{x}, \mathbf{p}) = \frac{1}{e^{-P(X) \cdot U(X)/T_H(X)} - 1} \quad (3.34)$$

is a solution to the Boltzmann equation in the presence of the time dependent perturbation, where

$$T_H(X)\sqrt{-g_{00}(X)} = \text{Const}, \quad T_H(x) = T_o \left( 1 - \frac{1}{2}H(X) \right), \quad (3.35)$$

and  $U_H^\mu(X) = (1/\sqrt{-g_{00}(X)}, 0, 0, 0)$ . This is true even if the temporal and spatial variations of  $H(X)$  are short compared to the mean free path,  $\sim 1/g^4 T$ . Note that in the distribution function  $n_p^H(t, \mathbf{x}, \mathbf{p})$ , the combination  $P \cdot U$  is

$$-P \cdot U(X) = \frac{-P_0(X)}{\sqrt{-g_{00}(X)}} = \sqrt{p^i(\delta_{ij} + H(X)\delta_{ij})p^j + m^2(T_H(X))}, \quad (3.36)$$

since  $P^\mu P^\nu g_{\mu\nu} = -m^2(T_H(X))$ .

In the presence of a gravitational field and a nontrivial dispersion relation, the Boltzmann equation is

$$\frac{1}{E_{\mathbf{p}}} \left( P^\mu \frac{\partial}{\partial X^\mu} - \frac{1}{2} \frac{\partial m^2(X)}{\partial X^\mu} \frac{\partial}{\partial P_\mu} - \Gamma_{\mu\nu}^\lambda P^\mu P^\nu \frac{\partial}{\partial P^\lambda} \right) f(t, \mathbf{x}, \mathbf{p}) = C[f, \mathbf{p}]. \quad (3.37)$$

The mass term might be more recognizable as a force term

$$-\frac{1}{2E_{\mathbf{p}}} \frac{\partial m^2(X)}{\partial X^\mu} \frac{\partial f}{\partial P_\mu} = -\frac{\partial E_{\mathbf{p}}}{\partial \mathbf{x}} \frac{\partial f}{\partial \mathbf{p}}. \quad (3.38)$$

The need for this term when computing the bulk viscosity has been emphasized previously [53]. The mass depends on the distribution function, which in turn depends on space-time [32]

$$m^2(X) = g^2(\phi)C_A \phi(X), \quad \phi(X) \equiv \frac{2\nu g}{d_A} \int \frac{d^4 P^\mu \sqrt{-g}}{(2\pi)^4} \theta(P^0) 2\pi \delta(-P^2) f_{\mathbf{p}}. \quad (3.39)$$

In equilibrium,  $\phi = T^2/6$ . It is important to emphasize that in order for kinetic theory to be valid, the scale of variation of  $g_{\mu\nu}(X)$  must be long compared to  $\sim 1/g^2 T$  which is the time it takes to establish the quasi-particle mass. Thus the gravitational field may be considered constant in Eq. (3.39).

We will substitute a trial solution

$$f(t, \mathbf{x}, \mathbf{p}) = n_p^H(t, \mathbf{x}, \mathbf{p}) + \delta f(t, \mathbf{x}, \mathbf{p}), \quad (3.40)$$

and subsequently verify that  $\delta f$  is of order  $(c_s^2 - 1/3) \sim g^4$ . Therefore,  $\delta f$  may be neglected when determining the gluon mass to leading order. The mass is then simply the time dependent equilibrium mass

$$m^2(T_H(X)) \simeq m^2(T_o) - T^2 \frac{\partial m^2}{\partial T^2} \Big|_{T_o} H(X), \quad (3.41)$$

where for pure glue,  $m^2(T) = g^2(T)C_A T^2/6$  [32].

With this observation, we substitute Eq. (3.40) into Eq. (3.37) which leads (after careful algebra) to an equation of motion for  $\delta f$

$$(\partial_t + v_{\mathbf{p}} \cdot \partial_{\mathbf{x}}) \delta f - n_p(1 + n_p) \frac{\tilde{m}^2}{2E_{\mathbf{p}} T} \partial_t H = \mathcal{C}[\delta f, \mathbf{p}], \quad (3.42)$$

where

$$\tilde{m}^2 \equiv m^2 - T^2 \frac{\partial m^2}{\partial T^2} \Big|_{T=T_o} = -C_A \beta(g) \frac{T_o^2}{6}. \quad (3.43)$$

In this result, we have used the definition of the beta function

$$\beta(g) \equiv \mu^2 \frac{\partial g^2(\mu^2)}{\partial \mu^2} = -\frac{g^4}{16\pi^2} \left( \frac{11C_A}{3} - \frac{4}{3} N_f T_F \right). \quad (3.44)$$

Since the source term in Eq. (3.42) is proportional to the beta function, the equilibrium distribution  $n_p^H(t, \mathbf{x}, \mathbf{p})$  provides an exact solution of the Boltzmann equation in a conformal theory. In the presence of weak conformal breaking,  $\delta f$  is of order  $\sim g^4$ , and Eq. (3.42) can be solved numerically for  $\delta f/g^4 H$  using the same procedure as in the previous cases.

Once  $\delta f$  is determined, the stress tensor can be found. Here we will follow the analysis of Ref. [53] (see also [32, 54]) which determines the appropriate stress tensor in the presence of a nontrivial dispersion relation. The stress tensor is

$$T^\mu{}_\mu(X) = -e(T_H(X)) + 3\mathcal{P}(T_H(X)) - \nu_g \int \frac{d^3 \mathbf{p}}{(2\pi)^3} \frac{\tilde{m}^2}{E_{\mathbf{p}}} \delta f(X), \quad (3.45a)$$

*i.e.* for  $K \neq 0$ , we have

$$T^\mu{}_\mu(\omega, k) = -\frac{1}{2} \left[ T \frac{\partial}{\partial T} (-e + 3\mathcal{P}) \right]_{T_o} H(\omega, k) - \frac{1}{2} \left[ \nu_g \int \frac{d^3 \mathbf{p}}{(2\pi)^3} \frac{\tilde{m}^2}{E_{\mathbf{p}}} \frac{\delta f(\omega, k)}{H(\omega, k)/2} \right] H(\omega, k). \quad (3.45b)$$

The term in square brackets is  $\eta_{\mu\nu}\eta_{\alpha\beta}G_R^{\mu\nu\alpha\beta}(\omega, k)$ . We note that it is the ‘‘tilde’’ mass that appears in Eq. (3.45a) making the correlator second order in the conformal breaking parameter. Fig. 2(d) shows the bulk spectral function and exhibits both rich hydrodynamic structure and a broad response.

The hydrodynamic prediction is found as follows. Around the equilibrium stress tensor, there is a small correction

$$T^{\mu\nu}(X) = \left[ e(T_H(X)) + \mathcal{P}(T_H(X)) \right] U_H^\mu U_H^\nu + \mathcal{P}(T_H(X)) g^{\mu\nu}(X) + \delta T^{\mu\nu}, \quad (3.46)$$

which in kinetic theory is given by

$$\delta T^{\mu\nu} = \int_{\mathbf{p}} \frac{p^\mu p^\nu}{E_{\mathbf{p}}} \delta f. \quad (3.47)$$

However, in the hydrodynamic regime the full stress tensor is parameterized by  $e(t, \mathbf{x})$  and  $U^\mu$  with

$$e(t, \mathbf{x}) = e(T_H(X)) + \epsilon(t, \mathbf{x}) \simeq e_o - \frac{1}{2} T c_v H(t, \mathbf{x}) + \epsilon(t, \mathbf{x}), \quad (3.48)$$

$$U^\mu(X) = U_H^\mu(X) + \delta U^\mu(X) \simeq \left( 1 - \frac{1}{2} H(t, \mathbf{x}), u^i(t, \mathbf{x}) \right). \quad (3.49)$$

Substituting these expressions into the conservation laws (Eq. (3.16) and Eq. (3.17)) yields the linearized equations of motion after careful algebra

$$\partial_t \epsilon + (e_o + \mathcal{P}_o) \partial_i u^i = \frac{1}{2} T c_v \partial_t H (1 - 3c_s^2), \quad (3.50)$$

$$(e_o + \mathcal{P}_o) \partial_t u^i + \partial_j \tau^{ji} = 0, \quad (3.51)$$

where the tensor  $\tau^{ij}$  is

$$\tau^{ij} = c_s^2 \epsilon \delta^{ij} - 2\eta \langle \partial^i u^j \rangle - \zeta \delta^{ij} \partial_l u^l - \frac{3}{2} \zeta \partial_t H \delta^{ij}. \quad (3.52)$$

In determining these equations we have used the relation,  $c_s^2 = (e_o + \mathcal{P}_o)/T c_v$ . In solving these equations, we can work to lowest order in the deviation from conformality,  $c_s^2 - 1/3$ . Noting that  $\zeta \sim (c_s^2 - 1/3)^2$  [36], while the deviations  $\epsilon(t, \mathbf{x})$  and  $u^l(t, \mathbf{x})$  are of order  $(c_s^2 - 1/3)$ , we determine  $T^\mu{}_\mu(\omega, k)$  to leading order in  $(c_s^2 - 1/3)$  for  $K \neq 0$

$$T^\mu{}_\mu(\omega, k) = -\frac{1}{2} \left[ T \frac{\partial}{\partial T} (-e + 3\mathcal{P}) \right]_{T_o} H(\omega, k) + (-1 + 3c_s^2) \epsilon(\omega, k) + \frac{9}{2} i \omega \zeta H(\omega, k). \quad (3.53)$$

Solving for  $\epsilon(t, \mathbf{x})$  from Eq. (3.50), substituting this result into  $T^\mu{}_\mu$ , and finally comparing to Eq. (3.45b), we determine the hydrodynamic prediction for this correlator

$$\eta_{\mu\nu}\eta_{\alpha\beta}G_R^{\mu\nu\alpha\beta}(\omega, k) = (1 - 3c_s^2)^2 T c_v \frac{-\omega^2 - i\Gamma_s \omega k^2}{\omega^2 - (c_s k)^2 + i\Gamma_s \omega k^2} - 9i\omega\zeta. \quad (3.54)$$

Using the thermodynamic result

$$(1 - 3c_s^2)^2 T c_v = \left( 3s \frac{\partial}{\partial s} - T \frac{\partial}{\partial T} \right) (-e + 3\mathcal{P}), \quad (3.55)$$

the imaginary part can be written

$$\eta_{\mu\nu}\eta_{\alpha\beta}\frac{\rho^{\mu\nu\alpha\beta}(\omega, k)}{2\omega} = \left(3s\frac{\partial}{\partial s} - T\frac{\partial}{\partial T}\right)(-e + 3\mathcal{P})\frac{(c_s k)^2\Gamma_s k^2}{(\omega^2 - c_s^2 k^2)^2 + (\omega\Gamma_s^2 k^2)^2} + 9\zeta. \quad (3.56)$$

Thus as  $k \rightarrow 0$  the first term approaches a delta function

$$\eta_{\mu\nu}\eta_{\alpha\beta}\frac{\rho^{\mu\nu\alpha\beta}(\omega, k)}{2\omega} = \left(3s\frac{\partial}{\partial s} - T\frac{\partial}{\partial T}\right)(-e + 3\mathcal{P})\left[\frac{\pi}{2}\delta(\omega - c_s k) + \frac{\pi}{2}\delta(\omega + c_s k)\right] + 9\zeta, \quad (3.57)$$

in agreement with the previous analysis of Romatschke and Son [49]. This explains the sharp sound pole seen in Fig. 2(d).

The free streaming Boltzmann equation does not provide a good description of the asymptotic solution at large  $k$  and  $\omega$ . This is because the large  $k$  and large  $\omega$  limits do not commute with the  $\mathbf{p} \rightarrow 0$  limit; the bulk channel is sensitive to these soft momenta. Indeed if we neglect the collision term in Eq. (3.42), the “solution”,

$$\delta f(\omega, k) = \frac{\tilde{m}^2}{2E_p T} \frac{\omega H n_p (1 + n_p)}{\omega - v_{\mathbf{p}} \cdot \mathbf{k} + i\epsilon}, \quad (3.58)$$

does not obey the boundary condition  $\lim_{\mathbf{p} \rightarrow 0} \chi(\mathbf{p}) = 0$ , and the  $T^\mu_\mu$  computed with this “solution” is infrared divergent. Thus the free result is not shown in Fig. 2(d).

#### IV. COMPARISON WITH SECOND ORDER HYDRODYNAMICS

In the long wavelength limit the response of the linearized kinetic theory discussed in Section II can be described with linearized hydrodynamics, which is a systematic expansion in gradients. At leading order in the coupling, the microscopic dynamics described by this kinetic theory is conformal, and thus the appropriate hydrodynamic theory is conformal hydrodynamics [50, 55]. Beyond leading order in the coupling, there are corrections to the kinetic theory which break scale invariance, and a more general non-conformal hydrodynamic theory must be used to characterize the long wavelength response of kinetic theory and gluodynamics more generally [56]. Indeed, in Section III E we determined the subleading non-conformal corrections to kinetic theory due to the scale dependence of medium masses and used this result to determine the bulk response function. Subsequently we analyzed this response with non-conformal hydrodynamics at first order.

In this section, we will first limit the discussion to leading order kinetic theory where the microscopic dynamics is conformal. We will analyze the sound and tensor channels with conformal hydrodynamics through second order following the fundamental work of Baier, Romatschke, Son, Starinets, and Stephanov (BRSSS) [50]. The goal here is to determine the  $k$  and  $\omega$  where the second order theory ceases to be a good description of the dynamics. Subsequently we will analyze the bulk channel with non-conformal linearized hydrodynamics through second order and determine the relevant non-conformal transport coefficients.

##### A. The sound mode and conformal second order hydrodynamics

In conformal linearized hydrodynamics, the dissipative part of the stress tensor, which is conformally invariant and is second order in derivatives, is given by [50]

$$\pi_2^{\mu\nu} = \eta\tau_\pi \left[ 2u_\alpha R^{\alpha(\mu\nu)\beta} u_\beta - 2\langle \nabla^\mu \nabla^\nu \ln T \rangle \right] + \kappa \left[ R^{\langle \mu\nu \rangle} - 2u_\alpha R^{\alpha\langle \mu\nu \rangle\beta} u_\beta \right], \quad (4.1)$$



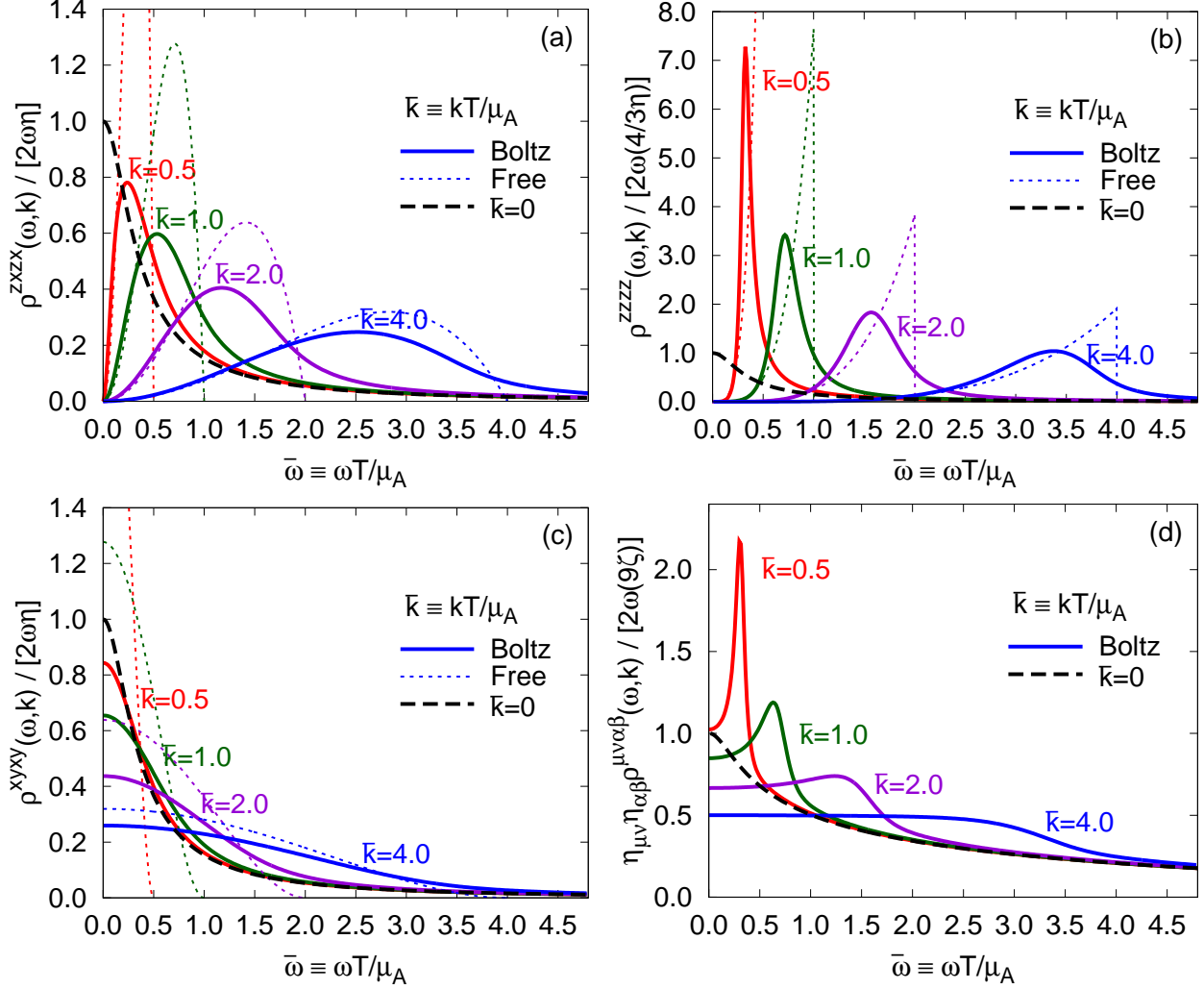


FIG. 2: The spectral density  $\rho(\omega) = -2 \text{Im} G_R(\omega, k)$  for the (a) shear mode  $G_R^{zzxx}(\omega, k)$ , (b) the sound mode  $G_R^{zzzz}(\omega, k)$ , (c) the tensor mode  $G^{xyxy}(\omega, k)$ , and (d) the bulk mode  $\eta_{\mu\nu}\eta_{\alpha\beta}G_R^{\mu\nu\alpha\beta}(\omega, k)$ . The solid lines show the complete results, while the dotted lines show the expectations of the free Boltzmann equation. The variables  $\omega$  and  $k$  are measured in units of  $\mu_A/T$ , with  $\mu_A = g^2 C_A m_D^2 / 8\pi \log(T/m_D)$ . The shear viscosity is  $\eta/(e+p) = 0.4613 T/\mu_A$  so that  $\bar{\omega} = 0.5, 1.0, 2.0, 4.0$  corresponds to  $\omega \eta / [(e+p)c_s^2] \simeq 0.7, 1.4, 2.8, 5.6$ , as chosen in Fig. 4.

where  $R^{\alpha\mu\nu\beta}$  ( $R^{\mu\nu}$ ) is the Riemann (Ricci) tensor, and  $\tau_\pi$  and  $\kappa$  are new transport coefficients. Using the zeroth order equations of motion and the conformal dependence of  $\eta$  on temperature  $\eta \propto T^3$ , BRSSS rewrite the constituent relation as a dynamical equation for  $\pi^{\mu\nu}$

$$\pi^{\mu\nu} = \pi_1^{\mu\nu} - \tau_\pi \langle D\pi^{\mu\nu} \rangle + \kappa \left[ R^{\langle\mu\nu\rangle} - 2u_\alpha R^{\alpha\langle\mu\nu\rangle\beta} u_\beta \right]. \quad (4.2)$$

This equation is similar to the phenomenological model of Israel and Stewart [57, 58]. We will compare the static theory, which consists of  $\nabla_\mu T^{\mu\nu} = 0$  and a constituent relation (Eq. (4.1)), to the dynamical theory, which consists of  $\nabla_\mu T^{\mu\nu} = 0$  and a dynamical equation (Eq. (4.2)). We will see that although the two theories agree in the limit of validity, neither really reproduces the structure of kinetic theory for  $\omega, ck \gtrsim 0.8 [\eta/(e_o + \mathcal{P}_o)c_s^2]^{-1}$ , though the dynamical theory fares better for larger  $\omega$ .

In conformal second order hydrodynamics, the Green function of the tensor channel is determined by solving the equations of motion in the external field  $h_{xy}(t, z)$ . Following the procedure described above, we have [50]

$$G_R^{xyxy}(\omega, k) = -i\eta\omega + \tau_\pi\eta\omega^2 - \frac{1}{2}\kappa(\omega^2 + k^2). \quad (4.3)$$

When  $\omega = 0$ , the source term of the Boltzmann equation is zero (see Eq. (3.13)), while  $G^{xyxy}(0, k) = -\kappa k^2/2$ . Therefore,  $\kappa = 0$  in a theory based on the conformal Boltzmann equation to this order [55]. At higher orders  $\kappa$  is non-zero. Indeed,  $\kappa$  is determined by the  $k$  dependence of the static susceptibility

$$G_R^{xyxy}(0, k) = -i \int d^4X e^{i\mathbf{k}\cdot\mathbf{x}} \theta(t) \langle [T^{xy}(t, \mathbf{x}), T^{xy}(0, \mathbf{0})] \rangle' = -\frac{1}{2}\kappa k^2, \quad (4.4)$$

which may be calculated with straightforward perturbation theory. For pure glue this calculation has been done in perturbation theory and the result is non-zero,  $\kappa = d_A T^2/18$  [49]. Nevertheless, we see that  $\kappa$  is of order  $\sim T^2$ , and is significantly smaller than the other second order transport coefficient  $\eta\tau_\pi \sim T^2/g^8$  which can be determined by the linearized Boltzmann equation to this order. Specifically, we extract  $\eta\tau_\pi$  by examining the real part of the response function in the limit  $\omega \rightarrow 0$  at  $k = 0$ . For  $N_c = 3$  and various numbers of flavors in a leading log approximation we have:

$N_f$	0	2	3
$\tau_\pi/(\eta/sT)$	6.32	6.65	6.46

The details of the multicomponent plasma are presented later in Section V A.  $\tau_\pi$  has been determined previously in a complete leading order calculation in Ref. [55].

Now we will calculate the retarded Green function of the sound channel in two different ways. The conservation laws read

$$\begin{aligned} \partial_t \epsilon + (e_o + \mathcal{P}_o) \partial_z u^z &= -\frac{1}{2}(e_o + \mathcal{P}_o) \partial_t h_{zz}, \\ (e_o + \mathcal{P}_o) \partial_t u^z + c_s^2 \partial_z \epsilon + \partial_z \pi^{zz} &= 0. \end{aligned} \quad (4.5)$$

In the static theory, the constituent relation is

$$\pi^{zz} = -\frac{4}{3}\eta \partial_z u^z - \frac{2}{3}\eta \partial_t h_{zz} + \frac{2}{3}\eta \tau_\pi \partial_t^2 h_{zz} - \frac{4}{3}\eta \tau_\pi \frac{c_s^2}{(e_o + \mathcal{P}_o)} \partial_z^2 \epsilon - \frac{1}{3}\kappa \partial_t^2 h_{zz}, \quad (4.6)$$

while in the dynamic theory, Eq. (4.2) becomes

$$\tau_\pi \partial_t \pi^{zz} + \pi^{zz} = -\frac{2}{3}\eta \partial_t h_{zz} - \frac{4}{3}\eta \partial_z u^z - \frac{1}{3}\kappa \partial_t^2 h_{zz}. \quad (4.7)$$

Using the static formulation, we solve the equations of motion and find

$$G_R^{zzzz}(\omega, k) = (e_o + \mathcal{P}_o) \frac{c_s^2 \omega^2 - i\Gamma_s \omega^3 + \tau_\pi \Gamma_s \omega^4 + \tau_\pi \Gamma_s c_s^2 k^2 \omega^2 - \frac{2}{3}\kappa/(e_o + \mathcal{P}_o) \omega^4}{\omega^2 - c_s^2 k^2 + i\Gamma_s \omega k^2 - \tau_\pi \Gamma_s c_s^2 k^4} \quad (\text{static}). \quad (4.8)$$

In the dynamic theory, we find

$$G_R^{zzzz}(\omega, k) = (e_o + \mathcal{P}_o) \frac{c_s^2 \omega^2 - i\Gamma_s \omega^3 - i\tau_\pi c_s^2 \omega^3 - \frac{2}{3}\kappa/(e_o + \mathcal{P}_o) \omega^4}{\omega^2 - c_s^2 k^2 + i\Gamma_s \omega k^2 + i\tau_\pi c_s^2 \omega k^2 - i\tau_\pi \omega^3} \quad (\text{dynamic}). \quad (4.9)$$

The dispersion relations for the static and dynamic theories are

$$\omega^2 - c_s^2 k^2 + i\Gamma_s \omega k^2 - \tau_\pi \Gamma_s c_s^2 k^4 = 0 \quad (\text{static}), \quad (4.10)$$

$$\omega^2 - c_s^2 k^2 + i\Gamma_s \omega k^2 + i\tau_\pi c_s^2 \omega k^2 - i\tau_\pi \omega^3 = 0 \quad (\text{dynamic}). \quad (4.11)$$

In the static theory, the dispersion relation has only two solutions

$$\omega = \pm c_s k - \frac{i}{2} \Gamma_s k^2 \mp \frac{\Gamma_s}{2} \left( \frac{\Gamma_s}{4c_s} - \tau_\pi c_s \right) k^3 + \mathcal{O}(k^4). \quad (4.12)$$

By contrast, the dispersion relation in the dynamic theory has the two physical solutions of Eq. (4.12), and an extra solution

$$\omega = -\frac{i}{\tau_\pi} + \mathcal{O}(k^2). \quad (4.13)$$

Since  $\omega$  remains constant as  $k \rightarrow 0$ , this last solution lies beyond the hydrodynamic approximation [50].

Fig. 3 compares the full spectral density of sound channel with first and second order hydrodynamics. For  $\omega, ck \lesssim 0.35 [\eta/(e_o + \mathcal{P}_o)c_s^2]^{-1}$ , first order hydrodynamics does a reasonable job at capturing the dynamics. The second order theory does a good job for this entire range, and continues to work qualitatively until

$$\omega, ck \lesssim 0.7 [\eta/(e_o + \mathcal{P}_o)c_s^2]^{-1}. \quad (4.14)$$

For still larger  $k$ , the dynamic second order theory becomes too reactive, while the static second order theory becomes too diffusive. Nevertheless, the dynamic theory seems to capture some aspects of the high frequency response better than the static theory. All hydrodynamic simulations so far have been based on the dynamical theory, which is hyperbolic and causal [9].

## B. The bulk mode and non-conformal hydrodynamics at second order

Now we will perform a similar analysis of the bulk mode, which must be analyzed with non-conformal second order hydrodynamics [56]. In non-conformal linearized hydrodynamics the shear strain to second order is

$$\pi^{\mu\nu} = \pi_1^{\mu\nu} + \eta\tau_\pi \langle D\sigma^{\mu\nu} \rangle + \kappa \left[ R^{\langle\mu\nu\rangle} - 2u_\alpha R^{\alpha\langle\mu\nu\rangle\beta} u_\beta \right] + \kappa^* 2u_\alpha R^{\alpha\langle\mu\nu\rangle\beta} u^\beta, \quad (4.15)$$

while the bulk tensor can be written

$$\Pi = \Pi_1 + \zeta\tau_\pi D(\nabla \cdot u) + \xi_5 R + \xi_6 u_\alpha u_\beta R^{\alpha\beta}. \quad (4.16)$$

We will show that the non-conformal couplings to the  $R^{\mu\nu\alpha\beta}$  (*i.e.*  $\kappa^*, \xi_5, \xi_6$ ) all vanish to the order considered here. As with  $\kappa$  discussed above these couplings are determined by static susceptibilities. To see this, we turn on a static gravitational field

$$g_{\mu\nu}(\mathbf{x}) = (1 + H(\mathbf{x}))\eta_{\mu\nu} + \text{diag}(0, h(\mathbf{x}), h(\mathbf{x}), h(\mathbf{x})). \quad (4.17)$$

Substituting this form into the hydrodynamic equations, we compute a particular combination of the stress tensor components

$$\langle 2T^{zz}(k) - (T^{xx}(k) + T^{yy}(k)) \rangle = [2\kappa^* k^2] H(k) + [\kappa k^2] h(k). \quad (4.18)$$

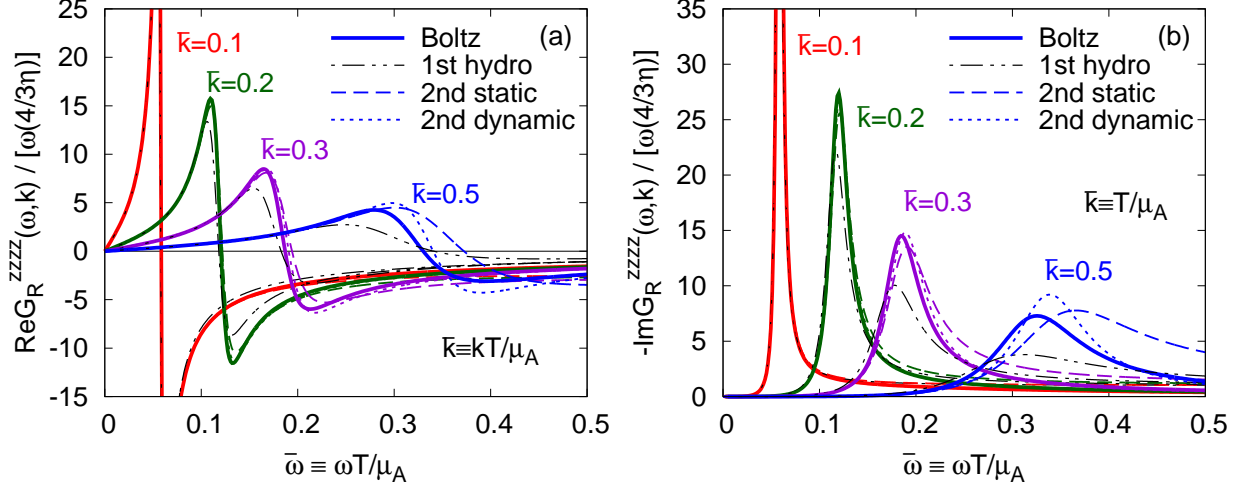


FIG. 3: (Color Online) The (a) real and (b) imaginary parts of the retarded Green function in the sound channel,  $G_R^{zzzz}(\omega, k)$ . The thick solid lines of various colors show the full numerical results from the Boltzmann equation; the thin dashed-dotted black lines show the prediction of the first order Navier-Stokes equations; the dashed lines show the prediction of the static second order theory (where  $\pi^{\mu\nu}$  is determined by the constituent relation, Eq. (4.1)); the dotted lines show the prediction of the dynamic second order theory (where  $\pi^{\mu\nu}$  is determined by a relaxation equation, Eq. (4.2)). The shear viscosity is  $\eta/(e+p) = 0.4613 T/\mu_A$  so that  $\bar{\omega} = 0.1, 0.2, 0.3, 0.5$  corresponds to  $\omega \eta/[(e+p)c_s^2] \simeq 0.14, 0.28, 0.42, 0.7$ .

Similarly, we define

$$\mathcal{O}_{\text{bulk}}(t, \mathbf{x}) = 3c_s^2 T_0^0(t, \mathbf{x}) + T_i^i(t, \mathbf{x}),$$

as was motivated in Ref. [53], and note that in the static gravitational field described above

$$\langle \mathcal{O}_{\text{bulk}}(k) \rangle = \left[ 9\xi_5 k^2 - \frac{3}{2}\xi_6 k^2 \right] H(k) + [6\xi_5 k^2] h(k). \quad (4.19)$$

Thus, all of the non-conformal couplings to the curvature tensor are related to the static susceptibilities

$$-i \int d^4 X e^{i\mathbf{k}\cdot\mathbf{x}} \theta(t) \langle [2T^{zz}(t, \mathbf{x}) - T^{xx}(t, \mathbf{x}) - T^{yy}(t, \mathbf{x}), T_\mu^\mu(0, \mathbf{0})] \rangle' = 2\kappa^* k^2 \quad (4.20)$$

$$-i \int d^4 X e^{i\mathbf{k}\cdot\mathbf{x}} \theta(t) \langle [\mathcal{O}_{\text{bulk}}(t, \mathbf{x}), T_\mu^\mu(0, \mathbf{0})] \rangle' = 9\xi_5 k^2 - \frac{3}{2}\xi_6 k^2 \quad (4.21)$$

$$-i \int d^4 X e^{i\mathbf{k}\cdot\mathbf{x}} \theta(t) \langle [\mathcal{O}_{\text{bulk}}(t, \mathbf{x}), T_i^i(0, \mathbf{0})] \rangle' = 6\xi_5 k^2 \quad (4.22)$$

These may be computed with straightforward perturbation theory as was done for  $\kappa$  in Ref. [49]. Further, since  $T_\mu^\mu = \frac{\beta(g)}{2g^2} G_{\mu\nu} G^{\mu\nu}$ , every insertion of  $T_\mu^\mu$  brings at least two powers of  $g$ . Thus we estimate that

$$\kappa^* = \xi_5 = \xi_6 = 0 + O(g^2) \quad (4.23)$$

In the Boltzmann equation, this must be considered zero to the order we are working. Indeed, we see from Eq. (3.13) and Eq. (3.42) that the sources for  $\delta f$  induced by  $H(\mathbf{x})$  and  $h(\mathbf{x})$ ,

$$-n_p(1+n_p) \frac{\tilde{m}^2}{2E_p T} \partial_t H, \quad \text{and} \quad n_p(1+n_p) \frac{p^2}{2E_p T} \partial_t h, \quad (4.24)$$

vanish for time independent gravitational fields.

To determine the last remaining coefficient  $\tau_\Pi$ , we will consider a correlation function of  $\mathcal{O}_{\text{bulk}}(t, \mathbf{x})$

$$\eta_{\mu\nu} G_R^{\mathcal{O}\mu\nu}(\omega, k) = -i \int d^4 X e^{i\omega t - i\mathbf{k}\cdot\mathbf{x}} \theta(t) \langle [\mathcal{O}_{\text{bulk}}(t, \mathbf{x}), T^\mu{}_\mu(0, \mathbf{0})] \rangle, \quad (4.25)$$

which can be constructed by turning on a gravitational field  $g_{\mu\nu} = (1 + H(t, \mathbf{x}))\eta_{\mu\nu}$  and evaluating  $\langle \mathcal{O}_{\text{bulk}}(t, \mathbf{x}) \rangle$

$$\langle \mathcal{O}_{\text{bulk}}(\omega, k) \rangle = -\frac{1}{2} \eta_{\mu\nu} G_R^{\mathcal{O}\mu\nu}(\omega, k) H(\omega, k). \quad (4.26)$$

At  $\mathbf{k} = 0$ , we substitute  $g_{\mu\nu} = (1 + H(t))\eta_{\mu\nu}$  into the second order non-conformal hydrodynamic equations, and determine  $\langle \mathcal{O}_{\text{bulk}}(\omega, 0) \rangle$  when  $\xi_5 = \xi_6 = 0$

$$\langle \mathcal{O}_{\text{bulk}}(\omega, 0) \rangle = -\frac{1}{2} [-9i\zeta\omega + 9\zeta\tau_\Pi\omega^2] H(\omega, 0). \quad (4.27)$$

The quantity in square brackets is the hydrodynamic prediction for the response function and should be valid at small  $\omega$ . In kinetic theory we turn on  $g_{\mu\nu} = (1 + H(t, \mathbf{x}))\eta_{\mu\nu}$  and measure the response  $\mathcal{O}_{\text{bulk}}(\omega, \mathbf{k})$  as described in Section III

$$\mathcal{O}_{\text{bulk}}(\omega, k) = -\frac{1}{2} \left[ \nu_g \int \frac{d^3 \mathbf{p}}{(2\pi)^3} \frac{3c_s^2 \tilde{m}^2 - (1 - 3c_s^2)p^2}{E_{\mathbf{p}}} \frac{\delta f(\omega, k)}{H(\omega, k)/2} \right] H(\omega, k). \quad (4.28)$$

Comparing the functional form of our numerical results from kinetic theory to the hydrodynamic form at  $\mathbf{k} = 0$ , we determine  $\tau_\Pi$

$$\frac{N_f}{\tau_\Pi/\tau_\pi} \left| \begin{array}{c|c|c} 0 & 2 & 3 \\ \hline 0.510 & 0.548 & 0.554 \end{array} \right|. \quad (4.29)$$

Thus we see that the relaxation time of bulk perturbations is similar to the relaxation time of shear perturbations.

## V. EXTENSION TO QUARKS AND SPECTRAL DENSITIES OF $J^\mu$

So far we have only discussed and simulated the pure glue theory. In QCD, the quarks carry nearly half of the entropy. For this reason, it is important to extend the analysis to include quarks. However, we will see that to  $\sim 10\%$  accuracy, the overall shape of the  $T^{\mu\nu}$  spectral functions given above is unchanged. After including quarks, we determine the current-current correlation function in high temperature QCD.

### A. Extension to quarks

When quarks are added to the mix, the leading log Boltzmann equation becomes somewhat more involved. Each species is expanded as follows

$$\delta f^a = n_p (1 \pm n_p) \chi^a(\mathbf{p}). \quad (5.1)$$

The collision operator is best expressed in terms of the sum of the fermion and the anti-fermion distribution functions,  $\delta f^{q+\bar{q}} \equiv \delta f^q + \delta f^{\bar{q}}$ , and the corresponding difference,  $\delta f^{q-\bar{q}} \equiv \delta f^q - \delta f^{\bar{q}}$ . The gluon distribution evolves according to

$$(\partial_t + v_{\mathbf{p}} \cdot \partial_{\mathbf{x}}) \delta f^g(t, \mathbf{x}, \mathbf{p}) = \left[ \mathcal{C}_{\text{FPloss}}^g + \mathcal{C}_{\text{FPgain}}^g + \mathcal{C}_{qg}^g \right]. \quad (5.2)$$

Similarly, the  $q + \bar{q}$  distribution function obeys the equation

$$(\partial_t + v_{\mathbf{p}} \cdot \partial_{\mathbf{x}}) \delta f^{q+\bar{q}}(t, \mathbf{x}, \mathbf{p}) = \left[ (\mathcal{C}_{\text{FPloss}}^q + \mathcal{C}_{\text{FPloss}}^{\bar{q}}) + (\mathcal{C}_{\text{FPgain}}^q + \mathcal{C}_{\text{FPgain}}^{\bar{q}}) + (\mathcal{C}_{qg}^q + \mathcal{C}_{qg}^{\bar{q}}) \right]. \quad (5.3)$$

The corresponding Boltzmann equation for the fermion difference is simpler since the gain term for the Fokker Planck evolution cancels in the difference

$$(\partial_t + v_{\mathbf{p}} \cdot \partial_{\mathbf{x}}) \delta f^{q-\bar{q}}(t, \mathbf{x}, \mathbf{p}) = \left[ (\mathcal{C}_{\text{FPloss}}^q - \mathcal{C}_{\text{FPloss}}^{\bar{q}}) + (\mathcal{C}_{qg}^q - \mathcal{C}_{qg}^{\bar{q}}) \right]. \quad (5.4)$$

The ingredients here are the following:

1. The Fokker-Planck evolution loss term is

$$\mathcal{C}_{\text{FPloss}}^a[\chi; \mathbf{p}] = T\mu_a \frac{\partial}{\partial \mathbf{p}^i} \left( n_p(1 \pm n_p) \frac{\partial}{\partial \mathbf{p}^i} \left[ \frac{\delta f^a}{n_p(1 \pm n_p)} \right] \right), \quad (5.5)$$

where the species dependent drag coefficient is

$$\frac{d\mathbf{p}}{dt} = -\mu_a \hat{\mathbf{p}}, \quad \text{with} \quad \mu_a = \frac{g^2 C_{R_a} m_D^2}{8\pi} \log \left( \frac{T}{m_D} \right), \quad (5.6)$$

and the Debye mass

$$m_D^2 = \sum_a^{g\bar{f}} \frac{g^2 C_{R_a}}{d_A} \nu_a \int_{\mathbf{p}} \frac{n_p^a(1 \pm n_p^a)}{T} = \frac{g^2 T^2}{3} (N_c + N_f T_F). \quad (5.7)$$

$C_{R_a}$  is the quadratic Casimir of species  $a$ .

2. The gain terms are also similar to the previous section. The total diffusion current is

$$\mathbf{j}_{\mathbf{p}} = - \sum_a \nu_a T \mu_a n_p^a (1 \pm n_p^a) \frac{\partial \chi^a(\mathbf{p})}{\partial \mathbf{p}}, \quad (5.8)$$

which only involves the sum of fermion and anti-fermion flavors. The gain terms are

$$\mathcal{C}_{\text{FPgain}}^a = \frac{g^2 C_{R_a}}{T m_D^2 d_A} \left[ \frac{1}{p^2} \frac{\partial}{\partial p} p^2 n_p (1 \pm n_p) \right] \frac{dE}{dt} + \frac{g^2 C_{R_a}}{T m_D^2 d_A} \left[ \frac{\partial}{\partial \mathbf{p}} n_p (1 \pm n_p) \right] \cdot \frac{d\mathbf{P}}{dt}, \quad (5.9)$$

where  $dE/dt$  and  $d\mathbf{P}/dt$  are the total work and momentum transfer per volume on the hard particles, *i.e.* Eqs. (2.7) and (2.8) but with the current given by Eq. (5.8).

3. When quarks are present there are additional processes that transform quarks and anti-quarks to gluons (and vice versa) by scattering off the fermion mean field. For the fermion sum, the collision operator for this process is

$$\mathcal{C}_{qg}^q + \mathcal{C}_{qg}^{\bar{q}} = -2\gamma \frac{n_p^F(1 + n_p^B)}{p} [\chi^q(\mathbf{p}) + \chi^{\bar{q}}(\mathbf{p}) - 2\chi^g(\mathbf{p})], \quad (5.10)$$

where we have defined for subsequent use

$$\gamma \equiv \frac{g^4 C_F^2 \xi_{BF}}{4\pi} \log(T/m_D), \quad \xi_{BF} \equiv \int_{\mathbf{k}} \frac{n_k^F(1+n_k^B)}{k} = \frac{T^2}{16}. \quad (5.11)$$

The analogous gluon collision operator entering in Eq. (5.2) is

$$\mathcal{C}_{qq}^g = - \sum_q^f \frac{\nu_q}{\nu_g} (\mathcal{C}_{qq}^q + \mathcal{C}_{qq}^{\bar{q}}), \quad (5.12)$$

where the sum is over the light quark flavors.

4. For the fermion difference, we note that the Fokker-Planck evolution is the same as before, but the gain terms cancel when the difference is taken. The quarks and gluons scattering off the fermion mean field (*i.e.* diagrams D and E in Appendix A 2) yield the collision term

$$\begin{aligned} (\mathcal{C}_{qq}^q - \mathcal{C}_{qq}^{\bar{q}}) = & -2\gamma \frac{n_p^F(1+n_p^B)}{p} [\chi^q(\mathbf{p}) - \chi^{\bar{q}}(\mathbf{p})] \\ & + \frac{2\gamma}{\xi_{BF}} \frac{n_p^F(1+n_p^B)}{p} \int_{\mathbf{k}} \frac{n_k^F(1+n_k^B)}{k} [\chi^q(\mathbf{k}) - \chi^{\bar{q}}(\mathbf{k})], \end{aligned} \quad (5.13)$$

where the first line is the loss term and the second line is the gain term.

Using these formulas, the spectral functions computed in the last section can also be computed in multi-component plasmas – see Appendix B for details. We have found that when the response functions are expressed in terms of appropriately scaled kinematic variables

$$\bar{\omega} = \omega \frac{\eta}{(e_o + \mathcal{P}_o)c_s^2}, \quad \bar{k} = ck \frac{\eta}{(e_o + \mathcal{P}_o)c_s^2}, \quad (5.14)$$

the spectral densities are essentially unchanged in all channels. In Fig. 4(a), we show the bulk spectral function in terms of these scaled variables for three flavors and pure glue. The relative agreement between these curves indicates the dominance of the Fokker-Planck evolution in determining the shape of the response functions. In the next section, we will discuss spectral densities of  $J^\mu$ , where a similar scaling is observed if  $\omega$  and  $k$  are scaled by the diffusion coefficient, as seen in Fig. 4(b).

## B. Spectral densities of $J^\mu$

For simplicity and definiteness we will compute the current-current correlator of net strangeness. Since in a leading log approximation the susceptibilities and correlators are diagonal in flavor space, the flavor and electromagnetic spectral densities are trivially related to this result. To determine the strangeness response function, we will probe the Boltzmann equation with a fictitious flavor gauge field that couples only to the strangeness current.

In the framework of linear response, the average current in the presence of an external field is

$$\langle J^\mu(X) \rangle_A = +i \int d^4Y \theta(X^0 - Y^0) \langle [J^\mu(X), J^\nu(Y)] \rangle A_\nu(Y). \quad (5.15)$$

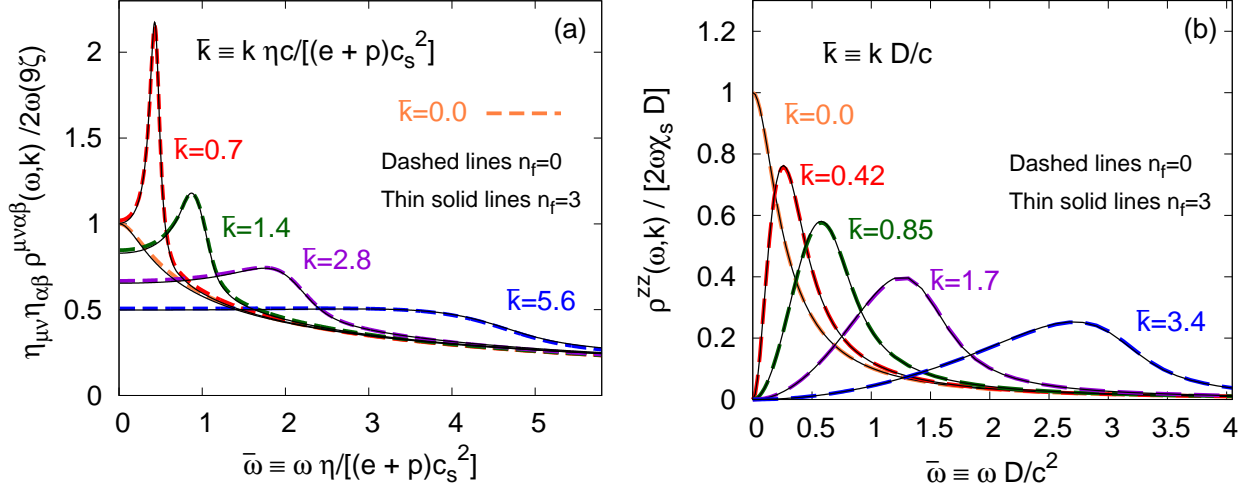


FIG. 4: (a) The bulk spectral function for three flavors compared to the pure glue theory. In this figure,  $\eta/(e_o + \mathcal{P}_o)$  is  $0.917T/\mu_A$  for  $N_f = 3$  and  $0.461T/\mu_A$  for  $N_f = 0$ , so that the  $k$  values for  $N_f = 0$  coincide with Fig. 2. (b) The longitudinal current-current spectral function for three flavors and the quenched approximation. In this figure  $D = 0.944T/\mu_F$  for  $N_f = 3$ , while  $D = 0.852T/\mu_F$  for  $N_f = 0$ , so that the  $k$  values for  $N_f = 0$  coincide with Fig. 5. The results are similar in the other channels.

In deriving this result, the definition of the current,  $J^\mu(X) = \delta S/\delta A^\mu(X)$ , is used to specify the interaction Hamiltonian,  $H_{\text{int}} = -\int d^3\mathbf{x} J^\mu A_\mu$ . In Fourier space we define

$$G_R^{\mu\nu}(\omega, \mathbf{k}) = -i \int d^4X e^{i\omega t - i\mathbf{k}\cdot\mathbf{x}} \theta(t) \langle [J^\mu(t, \mathbf{x}), J^\nu(0, 0)] \rangle, \quad (5.16)$$

and conclude that

$$\langle J^\mu(\omega, \mathbf{k}) \rangle_A = -G_R^{\mu\nu}(\omega, \mathbf{k}) A_\nu(\omega, \mathbf{k}). \quad (5.17)$$

Taking  $k$  along the  $z$  direction, there are two independent correlators,  $G_R^{zz}(\omega, k)$  and  $G_R^{xx}(\omega, k)$ .

To determine the Boltzmann equation in the presence of an external field, we note that the Lorentz force on a charged particle is  $\mathcal{F}^i = Q_a F_\mu^i v^\mu$ , which leads to the Boltzmann equation for the strangeness excess

$$\frac{1}{E_{\mathbf{p}}} \left( p^\mu \partial_\mu + Q_a F^{\mu\nu} p_\nu \frac{\partial}{\partial p^\mu} \right) f^a = C^a[f, \mathbf{p}], \quad (5.18)$$

where  $Q_s$  is one for strange quarks, minus one for anti-strange quarks, and zero for all other species. Turning on a weak gauge field  $A_\mu = (0, \mathbf{A})$  disturbs the system from equilibrium through the linearized Boltzmann equation

$$(-i\omega + iv_{\mathbf{p}} \cdot \mathbf{k}) \delta f^a(\omega, \mathbf{k}) - i\omega n_p (1 - n_p) Q_a A_i \frac{p^i}{E_{\mathbf{p}}} = C^a[\delta f, \mathbf{p}]. \quad (5.19)$$

We see that the gauge field does not disturb the fermion sum  $\delta f^{q+\bar{q}}$ , and only disturbs the fermion difference

$$(-i\omega + iv_{\mathbf{p}} \cdot \mathbf{k}) \delta f^{s-\bar{s}}(\omega, \mathbf{k}) - i\omega n_p (1 - n_p) 2Q_s A_i \frac{p^i}{E_{\mathbf{p}}} = C^{s-\bar{s}}[\delta f, \mathbf{p}]. \quad (5.20)$$



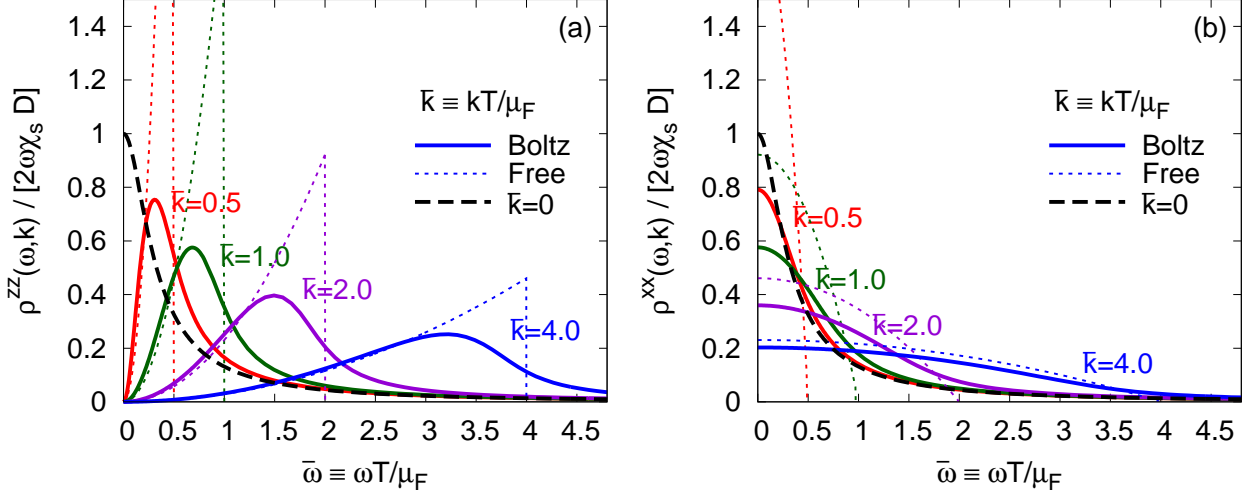


FIG. 5: (Color Online) The current-current correlator for  $N_c = 3$  and  $N_f = 0$  in the (a) longitudinal and (b) transverse channels.  $N_f = 0$  corresponds to the quenched approximation. In these  $\mathbf{k}$  points along the  $z$  direction, and  $\mu_F \equiv g^2 C_F m_D^2 \log(T/m_D)/8\pi$  is the drag coefficient of a quark in a leading log approximation. The diffusion coefficient is  $D = 0.852 T/\mu_F$ , so  $\bar{\omega} = 0.5, 1.0, 2.0, 4.0$  corresponds to  $\omega D/c^2 \simeq 0.42, 0.85, 1.7, 3.4$ , as chosen in Fig. 4. The thin dotted lines corresponding by color show the results from the free Boltzmann equation.

The full specification of the collision operator  $\mathcal{C}^{s-\bar{s}}$  is given in Eq. (5.13), and the numerical procedure used in the previous section is generalized to solve for  $\delta f^{s-\bar{s}}$  in Appendix B. Once  $\delta f$  is determined (or  $\delta f/Q_s A_z$  in practice), the current can be determined in a straightforward fashion

$$\langle J^i \rangle = Q_s \nu_s \int \frac{d^3 \mathbf{p}}{(2\pi)^3} \frac{p^i}{E_{\mathbf{p}}} \delta f^{s-\bar{s}}. \quad (5.21)$$

Through Eq. (5.17), this determines the current-current response function, which is illustrated in Fig. 5.

The spectral density for free Boltzmann equation explains the structure of the correlators at large  $\omega$  and  $k$ . Following what is by now standard procedure, we find:

$$\frac{\rho^{zz}(\omega, k)}{2\omega} = \frac{\pi Q_s^2 \nu_s \omega^2}{12 k^3} \theta(k - \omega), \quad (5.22a)$$

$$\frac{\rho^{xx}(\omega, k)}{2\omega} = \frac{\pi Q_s^2 \nu_s}{24 k} \left(1 - \frac{\omega^2}{k^2}\right) \theta(k - \omega), \quad (5.22b)$$

and we exhibit these free solutions in Fig. 5 with dashed lines. At zero  $k$ , the current-current correlator has been computed previously [29].

In the long wavelength limit, the current-current correlator is given by the diffusion equation which we will develop through second order. The current is expressed in terms of gradients of the net strangeness  $n_s(t, \mathbf{x})$  and the gauge field  $A^i(t, \mathbf{x})$ . For a linearized theory invariant under parity, the current to second order in the derivative expansion must have the following form

$$J_s^i = -D \partial^i n_s + \sigma E^i - (\sigma \tau_J) \partial_t E^i + \kappa_B (\nabla \times \mathbf{B})^i. \quad (5.23)$$

Here  $D$  is the diffusion coefficient,  $\sigma$  is the conductivity, and  $(\sigma \tau_J)$  and  $\kappa_B$  are new transport coefficients. In writing this expression, we have neglected the  $\epsilon^{ijk} \omega^j B^k$  and  $\mu \partial^i T$  which would

appear in magneto-hydrodynamics [59] (where  $B^i$  is not small) or at finite background chemical potential (where  $\mu$  is not small). Similarly, we have neglected  $n_s u^i$  which is non-linear in the small fluctuations of  $n_s(t, \mathbf{x})$  and  $u^i(t, \mathbf{x})$ . We also have used lower order equations of motion to recognize that  $\partial_t \partial^i n$  is actually third order in the derivative expansion.

In fact, the diffusion coefficient and the conductivity are simply related to each other. To see this, we first rewrite the constituent relation in terms of the chemical potential, and include one higher order term

$$J_s^i = -D\chi_s \partial^i \mu + \sigma E^i - (\sigma\tau_J) \partial_t E^i + \kappa_B (\nabla \times \mathbf{B})^i + [c_1 \chi_s \partial_t \partial^i \mu + \text{other higher order terms}] , \quad (5.24)$$

where  $\chi_s$  is the static susceptibility,

$$\chi_s = \frac{dn_s}{d\mu_s} = 2Q_s^2 \nu_s \frac{1}{T} \int_{\mathbf{p}} n_p (1 - n_p) = Q_s^2 \nu_s \frac{T^2}{6} . \quad (5.25)$$

Then we note that a perturbation of the form

$$\mu(X) + A_0(X) = \text{Const} \quad (5.26)$$

does not drive the system away from equilibrium, *i.e.*  $e^{-\beta(H-\mu N)}$  is constant. Thus all gradients in the constituent relation should involve the combination  $\partial^i(\mu + A_0)$ . This requirement forces a relation between the conductivity and the number diffusion coefficient

$$\chi_s D = \sigma , \quad (5.27)$$

and specifies the coefficient of one higher order term,  $c_1 = (D\tau_J)$ .

Now that the constituent relation is specified, the conservation laws  $\partial_t J^0 + \partial_i J^i = 0$  can be solved for  $J^0(\omega, k)$  in the presence of a sinusoidal electric field. Through the constituent relation (Eq. (5.23)) and linear response (Eq. (5.17)), this solution completely determines the form of the current-current correlator at small momenta

$$G^{zz}(\omega, k) = \frac{-\sigma\omega^2 - i(\sigma\tau_J)\omega^3}{-i\omega + Dk^2} , \quad (5.28a)$$

$$G^{xx}(\omega, k) = -i\omega\sigma + (\sigma\tau_J)\omega^2 - \kappa_B k^2 . \quad (5.28b)$$

When  $\omega = 0$ , the source term of the Boltzmann equation is zero (see Eq. (5.20)), while  $G^{xx}(0, k) = -\kappa_B k^2$ . Therefore,  $\kappa_B = 0$  in a theory based on the Boltzmann equation. (As in Section IV, this transport coefficient may be non-zero at higher order.) In the limit of  $\omega \rightarrow 0$  and  $k = 0$ , the real part of the Green function gives the value  $(\sigma\tau_J)$ . We tabulate this transport coefficient here (for  $N_c = 3$  and various numbers of flavors in a leading log approximation)

$N_f$	0	2	3
$\tau_J/D$	3.776	3.756	3.748

The imaginary part of Eq. (5.28a) describes the rapid ‘‘dip’’ seen at small  $\omega$  and  $k$  in Fig. 5(a). The second order theory also makes a definite prediction in Eq. (5.28a) for the form of the real part of the correlator at small  $\omega, k$ . This prediction is shown in Fig. 6, where it is compared to the first order theory and the full Boltzmann equation. The second order theory captures some aspects of the high frequency response.

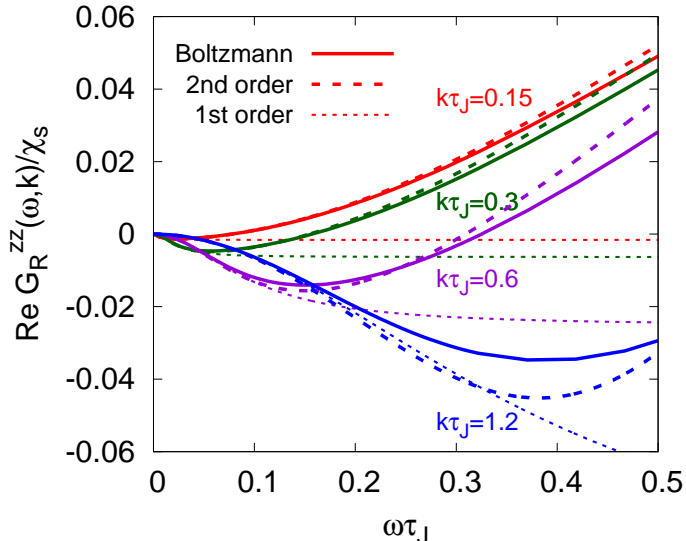


FIG. 6: (Color Online) The real part of the retarded current current response function for  $N_c = 3$  and  $N_f = 0$ . The thin dotted lines show the predictions of the first order diffusion equation, while the thick dashed lines show the prediction of the second order theory, Eq. (5.28a). Both are compared to the full Boltzmann equation.  $\omega$  and  $ck$  are in units of  $\tau_J^{-1} = 0.312 \mu_F/T$ . Thus  $k\tau_J = 0.15, 0.3, 0.6, 1.2$  corresponds to  $\omega T/\mu_F \simeq 0.045, 0.09, 0.18, 0.36$  in Fig. 5, *i.e.* smaller than the first Fig. 5 value.

We have written the “static” version of the second order diffusion equation. To the same order of accuracy, we can formulate a dynamic second order theory. Using the first order expression  $J_s^i = \sigma E^i - D \partial^i n_s$ , we can rewrite Eq. (5.23) (with  $\kappa_B = 0$ ) as

$$J_s^i = -D \partial^i n_s + \sigma E^i - \tau_J \partial_t J_s^i. \quad (5.29)$$

This is the canonical form of the telegraph equation, which has been extensively studied [60, 61], but we will not develop this connection further.

## VI. CONCLUSIONS

Fig. 2 shows our principle results for  $T^{\mu\nu}$  correlations in the shear, sound, bulk, and transverse tensor channels. These results are for pure glue theory, but in Section V A we determined how the Boltzmann equation would be modified when quarks are included. Fig. 4 shows how these modifications change the bulk and longitudinal current channels for various numbers of colors and flavors; the result is similar in the other channels. Fig. 5 shows our analogous results for  $J^\mu$  spectral densities in the transverse and longitudinal (*i.e.* the diffusion) channel.

In each channel (with the exception of the transverse tensor and transverse current), one sees a rich hydrodynamic structure at small momentum. We determined the hydrodynamic prediction through second order for these channels by solving the conservation laws in an external gravitational and electromagnetic fields. The electromagnetic response through second order has not been determined previously. Fig. 3 analyzes the sound channel in greater detail and compares the results to viscous hydrodynamics at first and second order to determine the range of validity of the macroscopic theory. (Fig. 6 shows an analogous study of charge diffusion.) Roughly, second order

hydrodynamics “works” up to about

$$\omega, ck \lesssim 0.7 \left[ \frac{\eta}{(e_o + \mathcal{P}_o)c_s^2} \right]^{-1}. \quad (6.1)$$

For larger momenta hydrodynamics becomes qualitatively wrong, and one sees a transition to free streaming quasi-particles (the dotted curves in Fig. 2 and Fig. 5). However, near the light cone  $\omega = k$ , the momenta need to be truly asymptotic before the sharp structures of the free theory are reproduced by the full result.

Nevertheless, already at fairly modest momenta, a smeared free result describes our full kinetic theory result fairly well. Consequently, it will be difficult to distinguish these curves in Euclidean space time as their integrals are the same. The question now is, when these smeared spectral shapes are combined with a reasonable model of the high frequency continuum, will the full spectral shape remain distinctly different from the completely smooth AdS/CFT results? We plan to make a complete comparison to the AdS/CFT and the lattice in future work, in an effort to see if quark and gluon quasi-particles can be distinguished in the lattice data.

In addition to providing definite predictions for the spectral densities, we hope that our analysis offers a new perspective on the linearized Boltzmann equation. In Section II and Appendix A, we have shown that close to equilibrium, the diffusive motion of the hard particles excess is described by a Fokker-Planck equation, which arises from the  $2 \rightarrow 2$  scattering graph. The work done during the Brownian process shows up as additional gain terms conserving energy and momentum. These gain terms have not appeared explicitly before, and they are essential to computing the spectral density or to simulating the Boltzmann equation. Ordinarily such a Fokker-Planck equation would conserve particle number. However, Bremsstrahlung processes, which are not logarithmically enhanced for typical momenta  $\mathbf{p} \sim T$ , can not be neglected in the limit  $\mathbf{p} \rightarrow 0$ . Consequently, the Fokker-Planck equation should be solved with an absorptive boundary condition at zero momentum – see Section II A 1 for further discussion. This has been understood previously through an analysis of the bulk viscosity [36], but has not been widely appreciated. In equilibrium (where particle number is constant), the particle loss from the temperature scale to the Debye scale through the absorptive boundary condition is compensated by the additional gain terms discussed above. A sample of evolution of a non-equilibrium distribution ultimately approaching equilibrium is given in Fig. 1.

The analysis and numerical work presented here sets the stage for simulating the jet-medium response in a leading log approximation. Work is in progress to extend the analysis further, and to simulate the jet-medium response in a complete leading order calculation.

## Acknowledgments

We gratefully acknowledge very useful discussions with Peter Arnold, Guy Moore, and Peter Petreczky. This work is supported by an OJI grant from the Department of Energy DE-FG-02-08ER4154 and the Sloan Foundation.

## Appendix A: Leading log analysis of the linearized Boltzmann equation

This section closely follows Ref. [46] and determines the leading-log Boltzmann equation for a pure glue theory. We will refer to diagrams A–D following the nomenclature of this work. Relative

to this work, the gain terms are explicitly given, and the final form emphasizes the Fokker Planck nature of the resulting theory.

## 1. Pure glue

Starting with Eq. (2.1), we linearize around the equilibrium distribution writing

$$f(t, \mathbf{x}, \mathbf{p}) = n_p + n_p(1 + n_p)\chi(t, \mathbf{x}, \mathbf{p}). \quad (\text{A1})$$

The full non-linear collision integral (including a final state symmetry factor) is<sup>3</sup>

$$C[f, \mathbf{p}] = - \int_{\mathbf{k}\mathbf{p}'\mathbf{k}'} \frac{1}{2} |M|^2 (2\pi)^4 \delta^4(P_{\text{tot}}) [f_{\mathbf{p}} f_{\mathbf{k}} (1 + f_{\mathbf{p}'}) (1 + f_{\mathbf{k}'}) - f_{\mathbf{p}'} f_{\mathbf{k}'} (1 + f_{\mathbf{p}}) (1 + f_{\mathbf{k}})] , \quad (\text{A2})$$

and this integral is subsequently linearized yielding

$$C[f, \mathbf{p}] = - \int_{\mathbf{k}\mathbf{p}'\mathbf{k}'} \frac{1}{2} |M|^2 (2\pi)^4 \delta^4(P_{\text{tot}}) n_p n_k (1 + n_{p'}) (1 + n_{k'}) [\chi(\mathbf{p}) + \chi(\mathbf{k}) - \chi(\mathbf{p}') - \chi(\mathbf{k}')] . \quad (\text{A3})$$

In the pure glue theory, the only diagram is  $t$ -channel gluon exchange, diagram A of Ref. [46]. The linearized integral can be recast as a variational problem

$$C[f, \mathbf{p}] = -(2\pi)^3 \frac{\delta}{\delta\chi(\mathbf{p})} I[\chi], \quad (\text{A4})$$

with

$$I[\chi] \equiv \frac{1}{16} \int_{\mathbf{p}\mathbf{k}\mathbf{p}'\mathbf{k}'} |M|^2 (2\pi)^4 \delta^4(P_{\text{tot}}) n_p n_k (1 + n_{p'}) (1 + n_{k'}) [\chi(\mathbf{p}) + \chi(\mathbf{k}) - \chi(\mathbf{p}') - \chi(\mathbf{k}')]^2 . \quad (\text{A5})$$

We classify the collision integrals as gain and loss terms

$$C[f, \mathbf{p}] = -(2\pi)^3 \frac{\delta}{\delta\chi(\mathbf{p})} (I[\chi]_{\text{loss}} + I[\chi]_{\text{gain}}) , \quad (\text{A6})$$

with

$$I[\chi]_{\text{loss}} = \int_{\mathbf{p}\mathbf{k}\mathbf{p}'\mathbf{k}'} |M|^2 (2\pi)^4 \delta^4(P_{\text{tot}}) n_p n_k (1 + n_{p'}) (1 + n_{k'}) \frac{2}{16} [\chi(\mathbf{p}) - \chi(\mathbf{p}')]^2 , \quad (\text{A7})$$

and

$$I[\chi]_{\text{gain}} = \int_{\mathbf{p}\mathbf{k}\mathbf{p}'\mathbf{k}'} |M|^2 (2\pi)^4 \delta^4(P_{\text{tot}}) n_p n_k (1 + n_{p'}) (1 + n_{k'}) \frac{2}{16} [\chi(\mathbf{p}) - \chi(\mathbf{p}')] [\chi(\mathbf{k}) - \chi(\mathbf{k}')] . \quad (\text{A8})$$

To extract the leading log, we expand in the momentum transfer<sup>4</sup>,  $\mathbf{q} = \mathbf{p}' - \mathbf{p}$ . In a leading log approximation, we can neglect the differences between  $k'$  and  $k$  and the collision integrals read

$$I[\chi]_{\text{loss}} = \int_{\mathbf{p}\mathbf{k}} n_p (1 + n_p) \frac{\partial\chi(\mathbf{p})}{\partial p^i} \frac{\partial\chi(\mathbf{p})}{\partial p^j} n_k (1 + n_k) I^{ij}(\mathbf{p}, \mathbf{k}) , \quad (\text{A9})$$

$$-I[\chi]_{\text{gain}} = \int_{\mathbf{p}\mathbf{k}} n_p (1 + n_p) \frac{\partial\chi(\mathbf{p})}{\partial p^i} \frac{\partial\chi(\mathbf{k})}{\partial k^j} n_k (1 + n_k) I^{ij}(\mathbf{p}, \mathbf{k}) , \quad (\text{A10})$$

<sup>3</sup> We will not write the spin and color information explicitly here. The matrix elements are summed over spins and colors associated with  $\mathbf{k}, \mathbf{p}', \mathbf{k}'$  and averaged over the spins and colors associated with  $\mathbf{p}$ . The distribution function  $f_{\mathbf{p}}$  is defined so that the total number of gluons is  $2d_A \int_{\mathbf{p}} f_{\mathbf{p}}$ .

<sup>4</sup> We have assumed that  $\mathbf{p}'$  is close  $\mathbf{p}$  and that  $t$  is small. For identical particles, there is an additional phase space region where  $\mathbf{k}'$  is close  $\mathbf{p}$  and  $u$  is small. This phase space region gives an equal contribution and this factor of two is included into the definition of  $I^{ij}$ .

where

$$I^{ij}(\mathbf{p}, \mathbf{k}) = \frac{1}{4} \int_{\mathbf{p}'\mathbf{k}'} (2\pi)^4 \delta^4(P + K - P' - K') |M|^2 \mathbf{q}^i \mathbf{q}^j. \quad (\text{A11})$$

We will subsequently show that in a leading log approximation  $I^{ij}(\mathbf{p}, \mathbf{k})$  evaluates to

$$I^{ij}(\mathbf{p}, \mathbf{k}) = \frac{T\mu_A}{2\xi_B} \left( \hat{\mathbf{p}}^i \hat{\mathbf{k}}^j + \hat{\mathbf{k}}^i \hat{\mathbf{p}}^j \right) + \frac{T\mu_A}{2\xi_B} (1 - \hat{\mathbf{p}} \cdot \hat{\mathbf{k}}) \delta^{ij}, \quad (\text{A12})$$

where we have defined the leading log coefficient in terms of the parameters  $\mu_A$  and  $\xi_B$  given in Eq. (2.4) and Eq. (2.10)

$$\frac{T\mu_A}{2\xi_B} = \frac{g^4 C_A^2 \nu_g}{16\pi d_A} \log(T/m_D). \quad (\text{A13})$$

Substituting  $I^{ij}$  into the loss term yields

$$I[\chi]_{\text{loss}} = \frac{1}{2} T\mu_A \int_{\mathbf{p}} n_p (1 + n_p) \frac{\partial \chi(\mathbf{p})}{\partial p^i} \frac{\partial \chi(\mathbf{p})}{\partial p^i}, \quad (\text{A14})$$

where we have used the rotational invariance of  $n_k(1 + n_k)$  and the definition  $\xi_B$ . The gain term is handled similarly yielding

$$\begin{aligned} -I[\chi]_{\text{gain}} &= \frac{T\mu_A}{2\xi_B} \left[ \int_{\mathbf{p}} n_p (1 + n_p) \hat{\mathbf{p}} \cdot \frac{\partial \chi(\mathbf{p})}{\partial \mathbf{p}} \right]^2 + \frac{T\mu_A}{2\xi_B} \left[ \int_{\mathbf{p}} n_p (1 + n_p) \frac{\partial \chi(\mathbf{p})}{\partial p^i} \right]^2 \\ &+ \frac{T\mu_A}{2\xi_B} \int_{\mathbf{p}\mathbf{k}} n_p n_k (1 + n_p)(1 + n_k) \left[ \hat{p}^j \hat{k}^i \frac{\partial \chi(\mathbf{p})}{\partial p^i} \frac{\partial \chi(\mathbf{k})}{\partial k^j} - \hat{\mathbf{p}} \cdot \hat{\mathbf{k}} \left( \frac{\partial \chi(\mathbf{p})}{\partial p^i} \right) \left( \frac{\partial \chi(\mathbf{k})}{\partial k^i} \right) \right]. \end{aligned} \quad (\text{A15})$$

The last line of this equation is in fact zero. To show this, we note that for the rotationally invariant  $n_k(1 + n_k)$  we have

$$\int_{\mathbf{k}} \frac{n_k(1 + n_k)}{k} \left[ k^i \frac{\partial \chi(\mathbf{k})}{\partial k^j} - k^j \frac{\partial \chi(\mathbf{k})}{\partial k^i} \right] = - \int_{\mathbf{k}} \left[ \left( k^i \frac{\partial}{\partial k^j} - k^j \frac{\partial}{\partial k^i} \right) \frac{n_k(1 + n_k)}{k} \right] \chi(\mathbf{k}) = 0. \quad (\text{A16})$$

This result can be used to interchange  $i$  and  $j$  in  $k^i \partial \chi(\mathbf{k}) / \partial k^j$  in  $I[\chi]_{\text{gain}}$ , yielding our final result

$$-I[\chi]_{\text{gain}} = \frac{T\mu_A}{2\xi_B} \left[ \int_{\mathbf{p}} n_p (1 + n_p) \hat{\mathbf{p}} \cdot \frac{\partial \chi(\mathbf{p})}{\partial \mathbf{p}} \right]^2 + \frac{T\mu_A}{2\xi_B} \left[ \int_{\mathbf{p}} n_p (1 + n_p) \frac{\partial \chi(\mathbf{p})}{\partial p^i} \right]^2. \quad (\text{A17})$$

Taking the variation of the gain and loss terms (as prescribed by Eq. (A6)) yields the linearized Boltzmann equation given in Section II.

#### a. A leading log integral

It remains to show that the integral Eq. (A11) actually equals Eq. (A12). To start, we note that since the matrix elements are symmetric in  $\mathbf{p}$  and  $\mathbf{k}$ , the integral must have the following form

$$I^{ij}(\mathbf{p}, \mathbf{k}) = a_1 \left( \hat{\mathbf{p}}^i \hat{\mathbf{p}}^j + \hat{\mathbf{k}}^i \hat{\mathbf{k}}^j \right) + a_2 \left( \hat{\mathbf{p}}^i \hat{\mathbf{k}}^j + \hat{\mathbf{k}}^i \hat{\mathbf{p}}^j \right) + a_3 \delta^{ij}. \quad (\text{A18})$$

To compute the coefficients of the basis we contract  $I^{ij}$  with, for instance,  $\hat{\mathbf{p}}^i \hat{\mathbf{p}}^j$ ,  $\hat{\mathbf{p}}^i \hat{\mathbf{k}}^j$  and  $\delta_{ij}$ . These integrals will be computed in the next paragraph and yield

$$\hat{\mathbf{p}}^i I^{ij} \hat{\mathbf{p}}^j = \frac{T\mu_A}{2\xi_B} (1 + \cos \theta_{pk}) = a_1(1 + \cos^2 \theta_{pk}) + 2a_2 \cos \theta_{pk} + a_3, \quad (\text{A19a})$$

$$\hat{\mathbf{p}}^i I^{ij} \hat{\mathbf{k}}^j = \frac{T\mu_A}{2\xi_B} (1 + \cos \theta_{pk}) = 2a_1 \cos \theta_{pk} + a_2(1 + \cos^2 \theta_{pk}) + a_3 \cos \theta_{pk}, \quad (\text{A19b})$$

$$I^{ii} = \frac{T\mu_A}{2\xi_B} (3 - \cos \theta_{pk}) = 2a_1 + 2a_2 \cos \theta_{pk} + 3a_3. \quad (\text{A19c})$$

Solving for  $a_1, a_2, a_3$  yields the result given in Eq. (A12).

To illustrate how the basis integrals are computed, we will compute  $\hat{\mathbf{p}}^i I^{ij} \hat{\mathbf{p}}^j$ . First, we use the three momentum delta function to perform the  $\mathbf{k}'$  integral and shift the integral over  $\mathbf{p}'$  to an integral over  $\mathbf{q}$ , *i.e.*  $\int_{\mathbf{p}'} \rightarrow \int_{\mathbf{q}}$ . Then we rotate our coordinate system so that  $\mathbf{p}$  points along the  $z$  axis and  $\mathbf{k}$  lies in the  $zx$  plane;  $\mathbf{q}$  is measured with respect to this coordinate system,  $d^3\mathbf{q} = q^2 dq d(c_{pq})d\phi$ . (Here and below, we use the shorthand notation  $c_{pq} = \cos \theta_{pq}$  and  $s_{pq} = \sin \theta_{pq}$ .) In these coordinates,  $\mathbf{p}, \mathbf{k}$  and  $\mathbf{q} \equiv \mathbf{p}' - \mathbf{p}$  are

$$\mathbf{p} = (0, 0, p), \quad (\text{A20a})$$

$$\mathbf{k} = (ks_{pk}, 0, kc_{pk}), \quad (\text{A20b})$$

$$\mathbf{q} = (qs_{qp} \cos \phi, qs_{qp} \sin \phi, qc_{qp}). \quad (\text{A20c})$$

The energy conservation  $\delta$ -function can be written

$$\delta(p + k - p' - k') = \frac{1}{q} \frac{1 - c_{pk}}{(1 - c_{pk})^2 + s_{pk}^2 \cos^2 \phi} \delta \left( c_{pq} - \frac{s_{pk} \cos \phi}{[(1 - c_{pk})^2 + s_{pk}^2 \cos^2 \phi]^{1/2}} \right), \quad (\text{A21})$$

where we have used  $p' \simeq p + q \cos \theta_{qp}$  and  $k' \simeq k + k \cos \theta_{kq}$ . The averaged matrix element (which appears in Eq. (A11)) in a leading log approximation is

$$\frac{1}{\nu_g} \sum_{s,c} |M|^2 = \frac{1}{16p^2 k^2 \nu_g} |\mathcal{M}|^2, \quad |\mathcal{M}|^2 = \frac{4\nu_g^2 g^4 C_A^2}{d_A} \frac{s^2}{t^2}, \quad (\text{A22})$$

where the Mandelstam invariants are

$$s = -(P + K)^2 = 2pk(1 - c_{pk}), \quad t = -(P' - P)^2 = -q^2 \frac{(1 - c_{pk})^2}{(1 - c_{pk})^2 + s_{pk}^2 \cos^2 \phi}. \quad (\text{A23})$$

Thus

$$\hat{\mathbf{p}}^i I^{ij}(\mathbf{p}, \mathbf{k}) \hat{\mathbf{p}}^j = \frac{1}{4} \int \frac{d^3q}{(2\pi)^3} |M|^2 2\pi \delta(p + k - p' - k') \hat{\mathbf{p}} \cdot \mathbf{q} \hat{\mathbf{p}} \cdot \mathbf{q}, \quad (\text{A24})$$

$$= \frac{\nu_g g^4 C_A^2}{8\pi d_A} \int \frac{dq}{q} \int \frac{d\phi}{2\pi} \frac{s_{pk}^2}{1 - c_{pk}} \cos^2 \phi = \frac{\nu_g g^4 C_A^2}{16\pi d_A} \log(T/m_D) (1 + c_{pk}). \quad (\text{A25})$$

The remaining integrals  $\hat{\mathbf{p}}^i I^{ij} \hat{\mathbf{k}}^j$  and  $I^{ii}$  are computed similarly yielding the results quoted in Eq. (A19).

## 2. Extension to multicomponent plasmas

We will be quite brief here since our results are to a certain extent simply a reanalysis of Ref. [46] along the lines of the previous section.

The Boltzmann equation is recast as a variational problem

$$C^a[f, \mathbf{p}] = -\frac{(2\pi)^3}{\nu_a} \frac{\delta}{\delta\chi^a(\mathbf{p})} I[\chi], \quad (\text{A26})$$

with<sup>5</sup>

$$I[\chi] \equiv \sum_{abcd} \frac{1}{16} \int_{\mathbf{p}\mathbf{k}\mathbf{p}'\mathbf{k}'} |M_{ab}^{cd}|^2 (2\pi)^4 \delta^4(P_{\text{tot}}) n_p^a n_k^b (1 \pm n_{p'}^c) (1 \pm n_{k'}^d) \left[ \chi^a(\mathbf{p}) + \chi^b(\mathbf{k}) - \chi^c(\mathbf{p}') - \chi^d(\mathbf{k}') \right]^2. \quad (\text{A27})$$

The collision integral is classified with gain and loss terms as in the previous section. The  $t$ -channel exchange diagrams (diagrams A–C) yield

$$I[\chi]_{A-C}^{\text{loss}} = \sum_{ab} \int_{\mathbf{p}\mathbf{k}\mathbf{p}'\mathbf{k}'} |M|^2 (2\pi)^4 \delta^4(P_{\text{tot}}) n_p^a n_k^b (1 \pm n_{p'}^a) (1 \pm n_{k'}^b) \frac{1}{4} \left[ \chi^a(\mathbf{p}) - \chi^a(\mathbf{p}') \right]^2, \quad (\text{A28})$$

where the invariant matrix elements are

$$|\mathcal{M}_{ab}^{ab}|^2 = 4\nu_a \nu_b \frac{g^4 C_{R_a} C_{R_b} s^2}{d_A t^2}. \quad (\text{A29})$$

Expanding the matrix elements as in the previous section (but keeping track of the species index) yields

$$I[\chi]_{A-C}^{\text{loss}} = \frac{T m_D^2}{16\pi} \log(T/m_D) \sum_a g^2 C_{R_a} \nu_a \int_{\mathbf{p}} n_p^a (1 \pm n_p^a) \left( \frac{\partial \chi^a(\mathbf{p})}{\partial p^i} \right)^2, \quad (\text{A30})$$

where we have used the definition of the Debye mass [18]

$$m_D^2 = \frac{1}{T d_A} \sum_b g^2 C_{R_b} \nu_b \int_{\mathbf{p}} n_k^b (1 \pm n_k^b). \quad (\text{A31})$$

The gain terms are handled as in the previous section

$$\begin{aligned} -I[\chi]_{A-C}^{\text{gain}} &= \frac{\log(T/m_D)}{16\pi d_A} \left[ \sum_a g^2 C_{R_a} \nu_a \int_{\mathbf{p}} n_p^a (1 \pm n_p^a) \hat{\mathbf{p}} \cdot \frac{\partial \chi^a(\mathbf{p})}{\partial \mathbf{p}} \right]^2 \\ &\quad + \frac{\log(T/m_D)}{16\pi d_A} \left[ \sum_a g^2 C_{R_a} \nu_a \int_{\mathbf{p}} n_p^a (1 \pm n_p^a) \frac{\partial \chi^a(\mathbf{p})}{\partial p^i} \right]^2. \end{aligned} \quad (\text{A32})$$

When fermions are included there is also a Compton and annihilation graph. First we will handle the annihilation graph. The annihilation graph substituted into Eq. (A27), can be written

<sup>5</sup> There is a slight difference between this and the previous section. In the last section, the matrix elements were averaged over the spins and colors of the particle  $a$ . Here the matrix element is summed over the spins and colors of particle  $a$ .



as sum of a loss and a gain term

$$I[\chi]_D^{\text{loss}} = \sum_q^f \frac{8}{16} \int_{\mathbf{p}\mathbf{k}\mathbf{p}'\mathbf{k}'} |M_{q\bar{q}}^{gg}|^2 (2\pi)^4 \delta^4(P_{\text{tot}}) n_p^q n_k^{\bar{q}} (1 + n_p^g) (1 + n_k^g) \times [(\chi^q(\mathbf{p}) - \chi^g(\mathbf{p}))^2 + (\chi^{\bar{q}}(\mathbf{k}) - \chi^g(\mathbf{k}))^2], \quad (\text{A33})$$

$$I[\chi]_D^{\text{gain}} = \sum_q^f \frac{8}{16} \int_{\mathbf{p}\mathbf{k}\mathbf{p}'\mathbf{k}'} |M_{q\bar{q}}^{gg}|^2 (2\pi)^4 \delta^4(P_{\text{tot}}) n_p^q n_k^{\bar{q}} (1 + n_p^g) (1 + n_k^g) \times [2(\chi^q(\mathbf{p}) - \chi^g(\mathbf{p}))(\chi^{\bar{q}}(\mathbf{k}) - \chi^g(\mathbf{k}))]. \quad (\text{A34})$$

The invariant matrix element is

$$|\mathcal{M}_{q\bar{q}}^{gg}|^2 \rightarrow 4\nu_q C_F^2 g^4 \left(\frac{u}{t}\right). \quad (\text{A35})$$

Then

$$I[\chi]_D^{\text{loss}} = \frac{1}{2} \sum_a^{\text{ff}} \int_{\mathbf{p}\mathbf{k}} n_p^F (1 + n_p^B) n_k^F (1 + n_k^B) (\chi^a(\mathbf{p}) - \chi^g(\mathbf{p}))^2 I(\mathbf{p}, \mathbf{k}), \quad (\text{A36})$$

where the integral

$$I(\mathbf{p}, \mathbf{k}) = \int_q |M|^2 2\pi \delta(P_{\text{tot}}^0) = \frac{\nu_q C_F^2 g^4}{4\pi p k} \log(T/m_D), \quad (\text{A37})$$

is easily performed using the parameterization given in the previous section. Then

$$I[\chi]_D^{\text{loss}} = \frac{1}{2} \gamma \sum_a^{\text{ff}} \nu_a \int_{\mathbf{p}} \frac{n_p^F (1 + n_p^B)}{p} (\chi^a(\mathbf{p}) - \chi^g(\mathbf{p}))^2, \quad (\text{A38a})$$

where we have used the symbols  $\gamma$  and  $\xi_{BF}$  given by Eq. (5.11). The gain term is handled similarly and yields

$$I[\chi]_D^{\text{gain}} = \sum_a^f \frac{\nu_a \gamma}{\xi_{BF}} \int_{\mathbf{k}} \frac{n_k^F (1 + n_k^B)}{k} (\chi^{\bar{a}}(\mathbf{k}) - \chi^g(\mathbf{k})) \int_{\mathbf{p}} \frac{n_p^F (1 + n_p^B)}{p} (\chi^a(\mathbf{p}) - \chi^g(\mathbf{p})). \quad (\text{A38b})$$

For the Compton process, we substitute the matrix element

$$|\mathcal{M}_{gq}^{ag}|^2 \simeq -4\nu_q C_F^2 g^4 \frac{s}{t} \quad (\text{A39})$$

into Eq. (A27), and read off the loss and gain terms

$$I[\chi]_E^{\text{loss}} = \sum_a^{\text{ff}} \frac{1}{2} \int_{\mathbf{p}\mathbf{k}\mathbf{p}'\mathbf{k}'} |M_{ga}^{ag}|^2 (2\pi)^4 \delta^4(P_{\text{tot}}) n_p^F n_k^B (1 + n_p^B) (1 - n_k^F) (\chi^a(\mathbf{p}) - \chi^g(\mathbf{p}))^2, \quad (\text{A40})$$

$$I[\chi]_E^{\text{gain}} = \sum_a^{\text{ff}} \frac{1}{2} \int_{\mathbf{p}\mathbf{k}\mathbf{p}'\mathbf{k}'} |M_{ga}^{ag}|^2 (2\pi)^4 \delta^4(P_{\text{tot}}) n_p^F n_k^B (1 + n_p^B) (1 - n_k^F) \quad (\text{A41})$$

$$\times [(\chi^a(\mathbf{p}) - \chi^g(\mathbf{p}))(\chi^g(\mathbf{k}) - \chi^a(\mathbf{k}))]. \quad (\text{A42})$$

The matrix element is simplified to

$$I[\chi]_E^{\text{loss}} = \frac{1}{2}\gamma \sum_a^{\text{ff}} \nu_a \int_{\mathbf{p}} \frac{n_p^F(1+n_p^B)}{p} [\chi^a(\mathbf{p}) - \chi^g(\mathbf{p})]^2, \quad (\text{A43a})$$

$$I[\chi]_E^{\text{gain}} = -\frac{1}{2} \frac{\gamma}{\xi_{BF}} \sum_a^{\text{ff}} \nu_a \left[ \int_{\mathbf{p}} \frac{n_p^F(1+n_p^B)}{p} (\chi^a(\mathbf{p}) - \chi^g(\mathbf{p})) \right]^2. \quad (\text{A43b})$$

Varying according  $I[\chi]$  with Eqs. (A30), (A32), (A38), and (A43), yields the results quoted in Section V A.

## Appendix B: Numerical solution

### 1. Pure glue

For our numerical solutions we introduce a real harmonic basis.

$$H_{lm}(\hat{\mathbf{p}}) = N_{lm} P_{|m|}(\cos \theta_{\mathbf{p}}) \times \begin{cases} 1 & \text{for } m = 0 \\ \sqrt{2} \cos m \phi_{\mathbf{p}} & \text{for } m > 0 \\ \sqrt{2} \sin |m| \phi_{\mathbf{p}} & \text{for } m < 0 \end{cases}, \quad (\text{B1})$$

where  $N_{lm}$  is the normalization factor

$$N_{lm} = \left[ \frac{2l+1}{4\pi} \frac{(l-|m|)!}{(l+|m|)!} \right]^{1/2}, \quad (\text{B2})$$

and  $P_{|m|}(\cos \theta_{\mathbf{p}})$  is the associated Legendre Polynomial defined without the Condon and Shortly phase. We note the equality

$$\hat{p}^z = \sqrt{\frac{4\pi}{3}} H_{10}(\hat{\mathbf{p}}), \quad \hat{p}^x = \sqrt{\frac{4\pi}{3}} H_{11}(\hat{\mathbf{p}}), \quad \hat{p}^y = \sqrt{\frac{4\pi}{3}} H_{1,-1}(\mathbf{p}). \quad (\text{B3})$$

For simplicity, we will first discuss the pure glue theory. The LHS ( $\times p^2$ ) of Eq. (3.13) in the harmonic basis becomes

$$p^2 \text{LHS} = (-i\omega \delta_{ll'} + ik C_{ll'}^m) N(p) \chi_{l'm} - i\omega N(p) \mathcal{H} S_{lm}(p), \quad (\text{B4})$$

where we have defined

$$N(p) = p^2 n_p (1 \pm n_p), \quad (\text{B5})$$

and recorded the Clebsch Gordan coefficients for  $k$  pointing in the  $z$  direction

$$C_{ll'}^m = \delta_{l+1,l'} \frac{N_{lm}}{N_{l+1,m}} \left( \frac{l-|m|+1}{2l+1} \right) + \delta_{l-1,l'} \frac{N_{lm}}{N_{l-1,m}} \left( \frac{l+|m|}{2l+1} \right). \quad (\text{B6})$$

In the source term,  $\mathcal{H}$  is one of the following

$$\mathcal{H} = h_{zx}, \frac{h_{zz}}{2}, h_{xy}, C_A \beta(g) T^2 \frac{H}{2}, \quad (\text{B7})$$

corresponding to the shear, sound, tensor, and bulk modes respectively. Examining Eq. (3.13) (for the first three modes) and Eq. (3.42) (for the bulk mode), we have the following translations:

$$-i\omega \frac{p^z p^z}{2E_p T} N(p) h_{zz} \rightarrow S_{lm}^{zz}(p) = \left( \delta_{l2} \delta_{m0} 2\sqrt{\frac{4\pi}{5}} + \delta_{l0} \delta_{m0} \sqrt{4\pi} \right) \frac{p}{3T}, \quad (\text{B8})$$

$$-i\omega \frac{p^z p^x}{E_p T} N(p) h_{zx} \rightarrow S_{lm}^{zx}(p) = \delta_{l2} \delta_{m1} \sqrt{\frac{4\pi}{15}} \frac{p}{T}, \quad (\text{B9})$$

$$-i\omega \frac{p^x p^y}{E_p T} N(p) h_{xy} \rightarrow S_{lm}^{xy}(p) = \delta_{l2} \delta_{m,-2} \sqrt{\frac{4\pi}{15}} \frac{p}{T}, \quad (\text{B10})$$

$$+i\omega \frac{\tilde{m}^2}{2E_p T} N(p) H \rightarrow S_{lm}^H(p) = \delta_{l0} \delta_{m0} \left( -\frac{\tilde{m}^2 \sqrt{4\pi}}{C_A \beta(g) T p} \right), \quad (\text{B11})$$

where  $\tilde{m}^2/T^2 C_A \beta(g)$  is given Eq. (B37).

Then Eq. (3.13) reads<sup>6</sup>

$$\begin{aligned} & (-i\omega \delta_{ll'} + ik C_{ll'}^m) N(p) \chi_{l'm} - i\omega N(p) \mathcal{H} S_{lm}(p) \\ &= T\mu_A \left[ \frac{\partial}{\partial p} N(p) \frac{\partial}{\partial p} - \frac{l(l+1)}{p^2} N(p) \right] \chi_{lm} + \frac{\delta_{l0} \delta_{m0}}{\xi_B} \sqrt{4\pi} \left[ -\frac{\partial N(p)}{\partial p} \right] \left( -\frac{dE}{dt} \right) \\ & \quad + \frac{\delta_{l1} \delta_{mm'}}{\xi_B} \sqrt{\frac{4\pi}{3}} \left[ -\frac{\partial N(p)}{\partial p} + \frac{2}{p} N(p) \right] \left( -\frac{dP}{dt} \right)_{1m'}. \end{aligned} \quad (\text{B12})$$

Our goal is to discretize momentum space so that the problem of finding  $\chi_{lm}(p_n)$  reduces to solving a system of linear equations

$$A_{ij} x_j = b_i. \quad (\text{B13})$$

To this end, the radial momenta are discretized,  $p_n = 0.5 \Delta p + n \Delta p$  with  $n = 0 \dots M-1$ . for numerical purposes we define

$$F_{lm} \equiv \frac{\chi_{lm}}{-i\omega \mathcal{H}}, \quad \mathbf{w} \equiv \frac{T\omega}{\mu_A}, \quad \mathbf{k} \equiv \frac{Tk}{\mu_A}, \quad (\text{B14})$$

and set  $T = 1$  from now on. Then the equation of motion becomes

$$\begin{aligned} & (-i\omega \delta_{ll'} + ik C_{ll'}^m) N(p) F_{l'm} + N(p) S_{lm}(p) \\ &= \left[ \frac{\partial}{\partial p} N(p) \frac{\partial}{\partial p} - \frac{l(l+1)}{p^2} N(p) \right] F_{lm} - \frac{\delta_{l0} \delta_{m0}}{\xi_{B,E}} \sqrt{4\pi} \left[ -\frac{\partial N(p)}{\partial p} \right] \left( \frac{1}{-i\omega \mathcal{H} \mu_A} \frac{dE}{dt} \right) + \\ & \quad - \frac{\delta_{l1} \delta_{mm'}}{\xi_{B,P}} \sqrt{\frac{4\pi}{3}} \left[ -\frac{\partial N(p)}{\partial p} + \frac{2}{p} N(p) \right] \left( \frac{1}{-i\omega \mathcal{H} \mu_A} \frac{dP}{dt} \right)_{1m'}, \end{aligned} \quad (\text{B15})$$

where we use a second order difference approximation for the second derivative

$$\frac{\partial}{\partial p} N(p) \frac{\partial F(p_n)}{\partial p} = \frac{1}{(\Delta p)^2} \left[ N(p_{n+1/2}) (F(p_{n+1}) - F(p_n)) - N(p_{n-1/2}) (F(p_n) - F(p_{n-1})) \right]. \quad (\text{B16})$$

<sup>6</sup> The forms of the  $dE/dt$  and  $dP/dt$  terms in this equation are chosen so that only  $N(p)$ , which is an analytic function, is differenced. Trial and error showed that this has the fastest approach to the continuum.

For the energy and momentum terms, we use a midpoint rule

$$\left( \frac{1}{-i\omega\mathcal{H}\mu_A} \frac{dE}{dt} \right) = \sqrt{4\pi} \sum_n \frac{\Delta p}{(2\pi)^3} p_n \frac{\partial}{\partial p} N(p_n) \frac{\partial F_{00}(p_n)}{\partial p}, \quad (\text{B17})$$

$$\left( \frac{1}{-i\omega\mathcal{H}\mu_A} \frac{dP}{dt} \right)_{1m} = \sqrt{\frac{4\pi}{3}} \sum_n \frac{\Delta p}{(2\pi)^3} p_n \left[ \frac{\partial}{\partial p} N(p_n) \frac{\partial F_{1m}(p_n)}{\partial p} - \frac{2}{p_n^2} N(p_n) F_{1m}(p_n) \right]. \quad (\text{B18})$$

The lattice definitions of  $\xi_B$  are defined so that energy and momentum are conserved

$$\xi_{B,E} = 4\pi \sum_n \frac{\Delta p}{(2\pi)^3} p_n \left[ -\frac{\partial N(p_n)}{\partial p} \right] \simeq \frac{1}{6}, \quad (\text{B19})$$

$$\xi_{B,P} = \frac{4\pi}{3} \sum_n \frac{\Delta p}{(2\pi)^3} p_n \left[ -\frac{\partial N(p_n)}{\partial p} + \frac{2}{p_n} N(p_n) \right] \simeq \frac{1}{6}, \quad (\text{B20})$$

and the derivative of the distribution function is

$$\frac{\partial N(p_n)}{\partial p} = \frac{N(p_{n+1/2}) - N(p_{n-1/2})}{\Delta p}. \quad (\text{B21})$$

The boundary conditions of the difference operator in Eq. (B16) need to be specified. The boundary condition discussed in Section II A 1,  $\chi(\mathbf{p})|_{\mathbf{p}=0} = 0$ , means that we take  $F_{00}(p_{-1}) = -F_{00}(p_0)$ ,  $F_{1m} = -F_{1m}(p_0)$ , and  $F_{lm}(p_{-1}) = F_{lm}(p_0)$  for  $l \geq 2$ . In Section II A 2, we wrote down a first order differential equation at high momentum, Eq. (2.18). In the spherical harmonic basis, this equation reads

$$\begin{aligned} (-i\omega\delta_{l'l'} + ikC_{l'l'}^m)N(p)F_{l'm}(p) + N(p)S_{lm}(p) &= -N(p)\frac{\partial F_{lm}}{\partial p} \\ -\frac{\delta_{l0}\delta_{m0}}{\xi_{B,E}}\sqrt{4\pi}N(p)\left(\frac{1}{-i\omega\mathcal{H}\mu_A}\frac{dE}{dt}\right) &- \frac{\delta_{l1}\delta_{mm'}}{\xi_{B,P}}\sqrt{\frac{4\pi}{3}}N(p)\left(\frac{1}{-i\omega\mathcal{H}\mu_A}\frac{dP}{dt}\right)_{1m'}. \end{aligned} \quad (\text{B22})$$

This first order differential equation leads to the update rule for the upper boundary

$$\begin{aligned} F_{lm}(p_M) &= F_{lm}(p_{M-1}) - \Delta p(-i\omega + ikC_{l'l'}^m)F_{l'm}(p_{M-1}) - \Delta p S_{lm}(p_{M-1}) \\ &- \Delta p \frac{\delta_{l0}\delta_{m0}}{\xi_{B,E}}\sqrt{4\pi}\left(\frac{1}{-i\omega\mathcal{H}\mu_A}\frac{dE}{dt}\right) - \Delta p \frac{\delta_{l1}\delta_{mm'}}{\xi_{B,P}}\sqrt{\frac{4\pi}{3}}\left(\frac{1}{-i\omega\mathcal{H}\mu_A}\frac{dP}{dt}\right)_{1m'}. \end{aligned} \quad (\text{B23})$$

We now wish to write the discretized form as the matrix equation,  $Ax = b$ . Examining the discretized update rules given in Eq. (B15) and Eq. (B16), and the boundary condition given in Eq. (B23), we see that the appropriate vector  $b_{nlm}$  is

$$b_{nlm} = N(p_n)S_{lm}(p_n) + \delta_{n,M-1}\frac{1}{(\Delta p)}N(p_{n+1/2})S_{lm}(p_n). \quad (\text{B24})$$

We note that the last  $\delta_{n,M-1}$  piece arises because in Eq. (B22) we are specifying the first derivative of the distribution function at high momentum.

In order to solve the system of linear equations, we used BiCGSTAB algorithm which generalizes the conjugate gradient algorithm to non-symmetric matrices [62]. In addition to performing the multiplication  $Ax$ , a typical BiCGSTAB implementation requires  $A^T x$ . In the present case,  $A^T x$  involves simply the replacement  $w \rightarrow -w$  and  $k \rightarrow -k$  in the equations. This is because only

the streaming term is the anti-symmetric part of the full matrix. Finally we should specify the preconditioner of the conjugate gradient algorithm. Here we simply take the diagonal matrix elements when viewed as a real matrix:

$$A_{\text{precond}} = \delta_{nlm,n'l'm'} \left[ -\frac{2N(p_n)}{(\Delta p)^2} - \frac{l(l+1)}{p^2} N(p_n) \right], \quad (\text{B25})$$

and this seems to provide satisfactory convergence. After solving for  $F_{lm}$ , the stress tensor is easily found – for example:

$$\frac{G^{zxzx}(\omega, k)}{-i\omega} \frac{\mu_A}{d_A T^5} = \frac{\delta T^{zx}(\omega, \mathbf{k})}{+i\omega h_{zx}} \frac{\mu_A}{d_A T^5}, \quad (\text{B26a})$$

$$= -2\sqrt{\frac{4\pi}{15}} \sum_n \frac{\Delta p}{(2\pi)^3} N(p_n) p_n F_{21}(p_n), \quad (\text{B26b})$$

$$\implies \eta \frac{\mu_A}{d_A T^5}, \quad (\text{B26c})$$

where the overall factor of two is the spin, and the arrow ( $\implies$ ) indicates the limit  $k = 0, \omega \rightarrow 0$ .

We record the final expressions for  $iG_R(\omega)/\omega$  for the sound channel, the tensor channel, and the bulk channel respectively

$$\frac{\delta T^{zz}(\omega, k)}{i\omega(h_{zz}/2)} \frac{\mu_A}{d_A T^5} = -2 \sum_n \frac{\Delta p}{(2\pi)^3} N(p_n) \frac{p_n}{3} \left( 2\sqrt{\frac{4\pi}{5}} F_{20}(p_n) + \sqrt{4\pi} F_{00}(p_n) \right), \quad (\text{B27a})$$

$$\implies \frac{4}{3} \eta \frac{\mu_A}{d_A T^5}, \quad (\text{B27b})$$

$$\frac{\delta T^{xy}(\omega, k)}{i\omega h_{xy}} \frac{\mu_A}{d_A T^5} = -2 \sum_n \frac{\Delta p}{(2\pi)^3} N(p_n) \left( p_n \sqrt{\frac{4\pi}{15}} \right) F_{2,-2}(p_n), \quad (\text{B27c})$$

$$\implies \eta \frac{\mu_A}{d_A T^5}, \quad (\text{B27d})$$

$$\frac{\delta T^\mu_\mu(\omega, k)}{i\omega(H/2)} \frac{\mu_A}{d_A T^5 C_A^2 \beta(g)^2} = -2 \sum_n \frac{\Delta p}{(2\pi)^3} N(p_n) \left( \frac{-\tilde{m}^2 \sqrt{4\pi}}{C_A \beta(g) p_n} \right) F_{00}(p_n), \quad (\text{B27e})$$

$$\implies 9\zeta \frac{\mu_A}{d_A T^5 C_A^2 \beta(g)^2}. \quad (\text{B27f})$$

Notice the pleasing similarity with the source terms in Eq. (B8).

## 2. Multi-component plasmas

Now we consider a multicomponent plasma. We introduce a rescaled Debye mass

$$\hat{m}_D^2 = \frac{m_D^2}{g^2 C_A} = \sum_a^{g, (q+\bar{q})/2} \hat{\nu}_a \hat{C}_a \int_{\mathbf{p}} n_p (1 \pm n_p) = \frac{1}{3} \left( 1 + \frac{N_f T_F}{N_c} \right), \quad (\text{B28})$$

where we have also rescaled the quadratic Casimir and the number of degrees of freedom

$$\hat{C}_a = \frac{C_{R_a}}{C_A}, \quad \hat{\nu}_a = \frac{\nu_a}{d_A}. \quad (\text{B29})$$

Explicitly we have  $\hat{\nu}_A = 2$ , and  $\hat{\nu}_q = 2N_f \frac{d_F}{d_A}$ , and  $\hat{\nu}_{(q+\bar{q})/2} = 4N_f d_F / d_A$ .

Then the total work and momentum transfer per volume are

$$\left( \frac{1}{-i\omega\mathcal{H}\mu_A d_A} \frac{dE}{dt} \right) = \sum_a^{g,(q+\bar{q})/2} \hat{\nu}_a \hat{C}_a \sqrt{4\pi} \sum_n \frac{\Delta p}{(2\pi)^3} p_n \frac{\partial}{\partial p} N(p_n, s_a) \frac{\partial F_{00}^a(p_n)}{\partial p}, \quad (\text{B30})$$

$$\left( \frac{1}{-i\omega\mathcal{H}\mu_A d_A} \frac{dP}{dt} \right)_{1m} = \sum_a^{g,(q+\bar{q})/2} \hat{\nu}_a \hat{C}_a \sqrt{\frac{4\pi}{3}} \sum_n \frac{\Delta p}{(2\pi)^3} p_n \times \left[ \frac{\partial}{\partial p} N(p_n, s_a) \frac{\partial F_{1m}^a(p_n)}{\partial p} - \frac{2}{p_n^2} N(p_n, s_a) F_{1m}^a(p_n) \right]. \quad (\text{B31})$$

The lattice versions of the rescaled Debye mass read

$$\hat{m}_{D,E}^2 \equiv \sum_a^{g,(q+\bar{q})/2} \hat{\nu}_a \hat{C}_a 4\pi \sum_n \frac{\Delta p}{(2\pi)^3} p_n \left[ -\frac{\partial N(p_n, s_a)}{\partial p} \right] \simeq \hat{m}_D^2, \quad (\text{B32a})$$

$$\hat{m}_{D,P}^2 \equiv \sum_a^{g,(q+\bar{q})/2} \hat{\nu}_a \hat{C}_a \frac{4\pi}{3} \sum_n \frac{\Delta p}{(2\pi)^3} p_n \left[ -\frac{\partial N(p_n, s_a)}{\partial p} + \frac{2}{p_n} N(p_n, s_a) \right] \simeq \hat{m}_D^2. \quad (\text{B32b})$$

The analogous equations of motion for  $a = g$  and  $a = (q + \bar{q})/2$  are

$$\begin{aligned} & (-i\omega\delta_{ll'} + ikC_{ll'}^m) N(p, s_a) F_{lm}^a + N(p, s_a) S_{lm}^a(p) \\ &= \hat{C}_a \left[ \frac{\partial}{\partial p} N(p, s_a) \frac{\partial}{\partial p} - \frac{l(l+1)}{p^2} N(p, s_a) \right] F_{lm}^a \\ & - \frac{\delta_{l0}\delta_{m0}\hat{C}_a}{\hat{m}_{D,E}^2} \sqrt{4\pi} \left[ -\frac{\partial N(p, s_a)}{\partial p} \right] \left( \frac{1}{-i\omega\mathcal{H}\mu_A d_A} \frac{dE}{dt} \right) \\ & - \frac{\delta_{l1}\delta_{mm'}\hat{C}_a}{\hat{m}_{D,P}^2} \sqrt{\frac{4\pi}{3}} \left[ -\frac{\partial N(p, s_a)}{\partial p} + \frac{2}{p} N(p, s_a) \right] \left( \frac{1}{-i\omega\mathcal{H}\mu_A d_A} \frac{dP}{dt} \right)_{1m'} + \frac{p^2 C_{gg}^a}{-i\omega\mathcal{H}\mu_A}. \end{aligned} \quad (\text{B33})$$

To specify the  $C_{qg}^a$  terms we define

$$\hat{\gamma} \equiv \frac{\gamma}{\mu_A} = 2 \left( \frac{C_F}{C_A} \right)^2 \frac{\xi_{BF}}{\hat{m}_D^2}, \quad \xi_{BF} \equiv \frac{1}{16}, \quad N_{BF} \equiv p n_p^F (1 + n_p^B). \quad (\text{B34})$$

Then the collision terms are

$$\frac{p^2}{-i\omega\mathcal{H}\mu_A} C_{qg}^{(q+\bar{q})/2} = -\hat{\gamma} N_{BF}(p_n) [2F_{lm}^{(q+\bar{q})/2}(p_n) - 2F_{lm}^g(p_n)], \quad (\text{B35a})$$

$$\frac{p^2}{-i\omega\mathcal{H}\mu_A} C_{qg}^g = \frac{\hat{\nu}_{(q+\bar{q})/2}}{\hat{\nu}_g} \hat{\gamma} N_{BF}(p_n) [2F_{lm}^{(q+\bar{q})/2}(p_n) - 2F_{lm}^g(p_n)]. \quad (\text{B35b})$$

Finally the expressions for the stress tensor remain valid with the appropriate modifications. For example, Eq. (B27e) becomes

$$\frac{\delta T^\mu_\mu(\omega, k)}{i\omega(H/2)} \frac{\mu_A}{d_A T^5 C_A^2 \beta(g)^2} = - \sum_a^{g,(q+\bar{q})/2} \hat{\nu}_a \sum_n \frac{\Delta p}{(2\pi)^3} N(p_n, s_a) \left( \frac{-\tilde{m}_a^2 \sqrt{4\pi}}{C_A \beta(g) p_n} \right) F_{00}^a(p_n), \quad (\text{B36a})$$

$$\implies 9\zeta \frac{\mu_A}{d_A T^5 C_A^2 \beta(g)^2}, \quad (\text{B36b})$$

where the scaled masses are

$$\frac{\tilde{m}_{(q+\bar{q})/2}^2}{C_A\beta(g)T^2} = -\frac{\hat{C}_F}{4}, \quad \frac{\tilde{m}_g^2}{C_A\beta(g)T^2} = -\left(\frac{1}{6} + \frac{\hat{\nu}_{(q+\bar{q})/2}\hat{C}_{(q+\bar{q})/2}}{24}\right). \quad (\text{B37})$$

In solving the linear system of equations, the transpose is also needed. When multiplying by  $A^T x$ , it must be realized that the matrix implied by Eq. (B35) is not symmetric, and the transpose of this equation should be used. Alternatively, Eq. (B35) can be made symmetric by rescaling  $F_{lm}^a$  with  $\sqrt{\nu_a}$  and changing the formulae of this section appropriately.

### 3. Charge diffusion

In this section we will outline a procedure to solve Eq. (5.20) numerically. As before we multiply by  $p^2$  and the left hand side becomes

$$p^2\text{LHS} = (-i\omega\delta_{ll'} + ikC_{ll'}^m) N(p)\chi_{l'm}(p) - i\omega N(p)\mathcal{A}S_{lm}(p), \quad (\text{B38})$$

where  $\mathcal{A}$  is one of

$$\mathcal{A} = \frac{2Q_s A_z}{T}, \quad \frac{2Q_s A_x}{T}. \quad (\text{B39})$$

In this section,  $N(p) = p^2 n_p(1 - n_p)$ , refers to the fermion distribution and we have dropped the  $s - \bar{s}$  label on  $\chi_{lm}^{s-\bar{s}}$ . From Eq. (5.20), we determine the corresponding sources:

$$-i\omega n_p(1 - n_p)2Q_s A_z \frac{p^z}{E_p T} \rightarrow S_{lm}^z = \sqrt{\frac{4\pi}{3}}\delta_{l1}\delta_{m0}, \quad (\text{B40a})$$

$$-i\omega n_p(1 - n_p)2Q_s A_x \frac{p^x}{E_p T} \rightarrow S_{lm}^x = \sqrt{\frac{4\pi}{3}}\delta_{l1}\delta_{m1}. \quad (\text{B40b})$$

For the net strangeness, we define  $F_{lm}$  in analogy with the previous section,  $F_{lm}(p) \equiv \frac{\chi}{-i\omega\mathcal{A}}$ . Eq. (5.20) becomes

$$\begin{aligned} & (-i\omega\delta_{ll'} + ikC_{ll'}^m) N(p)F_{l'm}(p) + N(p)S_{lm}(p) \\ &= \hat{C}_F \left[ \frac{\partial}{\partial p} N(p) \frac{\partial}{\partial p} - \frac{l(l+1)}{p^2} N(p) \right] F_{lm}(p) \\ & \quad - 2\hat{\gamma} N_{BF}(p) F_{lm}(p) - \frac{\delta_{l0}\delta_{m0}}{\xi_{BF,Q}} \sqrt{4\pi} N_{BF}(p) \left( \frac{1}{-i\omega\mathcal{A}} \frac{dQ}{dt} \right), \end{aligned} \quad (\text{B41})$$

where the charge transfer rate is

$$\frac{1}{-i\omega\mathcal{A}} \frac{dQ}{dt} = -2\hat{\gamma}\sqrt{4\pi} \sum_n \frac{\Delta p}{(2\pi)^3} N_{BF}(p_n) F_{00}(p_n). \quad (\text{B42})$$

We choose a lattice definition of  $\xi_{BF}$  so that the strange charge is exactly conserved

$$\xi_{BF,Q} = 4\pi \sum_n \frac{\Delta p}{(2\pi)^3} N_{BF}(p_n). \quad (\text{B43})$$

Finally, from Eq. (5.21) and the susceptibility Eq. (5.25) we determine the longitudinal and transverse current current correlators (or more precisely  $iG_R(\omega)/\omega$ ) in convenient units

$$\frac{J^z}{i\omega A^z} \frac{\mu_F}{T\chi_s} = -\frac{\hat{C}_F}{\xi_F} \sum_n \frac{\Delta p}{(2\pi)^3} N(p_n) \left( \sqrt{\frac{4\pi}{3}} F_{10}(p_n) \right) \implies D \frac{\mu_F}{T}, \quad (\text{B44a})$$

$$\frac{J^x}{i\omega A^x} \frac{\mu_F}{T\chi_s} = -\frac{\hat{C}_F}{\xi_F} \sum_n \frac{\Delta p}{(2\pi)^3} N(p_n) \left( \sqrt{\frac{4\pi}{3}} F_{11}(p_n) \right) \implies D \frac{\mu_F}{T}. \quad (\text{B44b})$$

- [1] K. Adcox *et al.* [PHENIX Collaboration], Nucl. Phys. A **757**, 184 (2005) [arXiv:nucl-ex/0410003].
- [2] J. Adams *et al.* [STAR Collaboration], Nucl. Phys. A **757**, 102 (2005) [arXiv:nucl-ex/0501009].
- [3] D. Molnar and M. Gyulassy, Nucl. Phys. A **697**, 495 (2002) [Erratum-ibid. A **703**, 893 (2002)] [arXiv:nucl-th/0104073].
- [4] D. Teaney, Phys. Rev. C **68**, 034913 (2003) [arXiv:nucl-th/0301099].
- [5] P. Romatschke and U. Romatschke, Phys. Rev. Lett. **99**, 172301 (2007) [arXiv:0706.1522 [nucl-th]].
- [6] H. Song and U. W. Heinz, Phys. Rev. C **77**, 064901 (2008) [arXiv:0712.3715 [nucl-th]].
- [7] K. Dusling and D. Teaney, Phys. Rev. C **77**, 034905 (2008) [arXiv:0710.5932 [nucl-th]].
- [8] Z. Xu and C. Greiner, Phys. Rev. C **79**, 014904 (2009) [arXiv:0811.2940 [hep-ph]].
- [9] For an overview see, D. A. Teaney, arXiv:0905.2433 [nucl-th], invited review for *QGP4*, editors R. C. Hwa and X. N. Wang.
- [10] G. Policastro, D. T. Son and A. O. Starinets, Phys. Rev. Lett. **87**, 081601 (2001) [arXiv:hep-th/0104066].
- [11] P. Kovtun, D. T. Son and A. O. Starinets Phys. Rev. Lett. **94**, 111601 (2005) [arXiv:hep-th/0405231]
- [12] J. P. Blaizot and E. Iancu, Phys. Rept. **359**, 355 (2002) [arXiv:hep-ph/0101103].
- [13] see for example, P. Arnold and L. G. Yaffe, Phys. Rev. D **57**, 1178 (1998) [arXiv:hep-ph/9709449].
- [14] see for example, D. T. Son and A. O. Starinets, Ann. Rev. Nucl. Part. Sci. **57**, 95 (2007) [arXiv:0704.0240 [hep-th]].
- [15] see for example, T. Schafer and D. Teaney, Rept. Prog. Phys. **72**, 126001 (2009) [arXiv:0904.3107 [hep-ph]].
- [16] P. Kovtun and A. Starinets, Phys. Rev. Lett. **96**, 131601 (2006) [arXiv:hep-th/0602059].
- [17] D. Teaney, Phys. Rev. D **74**, 045025 (2006) [arXiv:hep-ph/0602044].
- [18] see for example, M. Le Bellac, *Thermal Field Theory* (Cambridge University Press, 1996).
- [19] G. Aarts and J. M. Martinez Resco, JHEP **0204**, 053 (2002) [arXiv:hep-ph/0203177].



- [20] P. Petreczky and D. Teaney, Phys. Rev. D **73**, 014508 (2006) [arXiv:hep-ph/0507318].
- [21] K. Huebner, F. Karsch and C. Pica, “Correlation functions of the energy-momentum tensor in SU(2) gauge theory Phys. Rev. D **78**, 094501 (2008) [arXiv:0808.1127 [hep-lat]].
- [22] G. Aarts, C. Allton, J. Foley, S. Hands and S. Kim, Phys. Rev. Lett. **99**, 022002 (2007) [arXiv:hep-lat/0703008].
- [23] H. B. Meyer, Phys. Rev. D **76**, 101701 (2007) [arXiv:0704.1801 [hep-lat]].
- [24] M. Asakawa and T. Hatsuda, Phys. Rev. Lett. **92**, 012001 (2004) [arXiv:hep-lat/0308034].
- [25] A. Mocsy and P. Petreczky, Phys. Rev. Lett. **99**, 211602 (2007) [arXiv:0706.2183 [hep-ph]].
- [26] A. Jakovac, P. Petreczky, K. Petrov and A. Velytsky, Phys. Rev. D **75**, 014506 (2007) [arXiv:hep-lat/0611017].
- [27] H. B. Meyer, Nucl. Phys. A **830**, 641C (2009) [arXiv:0907.4095 [hep-lat]].
- [28] G. Aarts, C. Allton, J. Foley, S. Hands and S. Kim, PoS **LAT2006**, 134 (2006) [arXiv:hep-lat/0610061].
- [29] G. D. Moore and J. M. Robert, arXiv:hep-ph/0607172.
- [30] G. D. Moore and O. Saremi, JHEP **0809**, 015 (2008) [arXiv:0805.4201 [hep-ph]].
- [31] S. Caron-Huot, Phys. Rev. D **79**, 125009 (2009) [arXiv:0903.3958 [hep-ph]].
- [32] P. Arnold, G. D. Moore and L. G. Yaffe, JHEP **0301**, 030 (2003) [arXiv:hep-ph/0209353].
- [33] R. Baier, A. H. Mueller, D. Schiff and D. T. Son, Phys. Lett. B **502**, 51 (2001) [arXiv:hep-ph/0009237].
- [34] G. Baym, H. Monien, C. J. Pethick and D. G. Ravenhall, Phys. Rev. Lett. **64**, 1867 (1990).
- [35] P. Arnold, G. D. Moore and L. G. Yaffe, JHEP **0305**, 051 (2003) [arXiv:hep-ph/0302165].
- [36] P. Arnold, C. Dogan and G. D. Moore, Phys. Rev. D **74**, 085021 (2006) [arXiv:hep-ph/0608012].
- [37] S. Mrowczynski, Phys. Lett. B **314**, 118 (1993).
- [38] P. Arnold, J. Lenaghan and G. D. Moore, JHEP **0308**, 002 (2003) [arXiv:hep-ph/0307325].
- [39] A. H. Mueller, A. I. Shoshi and S. M. H. Wong, Phys. Lett. B **632**, 257 (2006) [arXiv:hep-ph/0505164].
- [40] A. Rebhan, P. Romatschke and M. Strickland, “Dynamics of quark-gluon plasma instabilities in discretized hard-loop JHEP **0509**, 041 (2005) [arXiv:hep-ph/0505261].
- [41] P. Arnold, G. D. Moore and L. G. Yaffe, Phys. Rev. D **72**, 054003 (2005) [arXiv:hep-ph/0505212].
- [42] P. Romatschke and R. Venugopalan, Phys. Rev. Lett. **96**, 062302 (2006) [arXiv:hep-ph/0510121].
- [43] B. Schenke, M. Strickland, A. Dumitru, Y. Nara and C. Greiner, Phys. Rev. C **79**, 034903 (2009) [arXiv:0810.1314 [hep-ph]].

- [44] B. Schenke, M. Strickland, C. Greiner and M. H. Thoma, Phys. Rev. D **73**, 125004 (2006) [arXiv:hep-ph/0603029].
- [45] H. Heiselberg, Phys. Rev. D **49**, 4739 (1994) [arXiv:hep-ph/9401309].
- [46] P. Arnold, G. D. Moore and L. G. Yaffe, JHEP **0011**, 001 (2000) [arXiv:hep-ph/0010177].
- [47] M. H. Thoma and M. Gyulassy, Nucl. Phys. A **544** (1992) 573C.
- [48] E. Braaten and M. H. Thoma, Phys. Rev. D **44**, 1298 (1991); *ibid.* Phys. Rev. D **44**, 2625 (1991).
- [49] P. Romatschke and D. T. Son, Phys. Rev. D **80**, 065021 (2009) [arXiv:0903.3946 [hep-ph]].
- [50] R. Baier, P. Romatschke, D. T. Son, A. O. Starinets and M. A. Stephanov, JHEP **0804**, 100 (2008) [arXiv:0712.2451 [hep-th]].
- [51] see for example, A. Hohenegger, A. Kartavtsev and M. Lindner, Phys. Rev. D **78**, 085027 (2008) [arXiv:0807.4551 [hep-ph]].
- [52] see for example, Hakan Andreasson, Living Rev. Relativity **8**, (2005) [<http://www.livingreviews.org/lrr-2005-2>].
- [53] S. Jeon and L. G. Yaffe, Phys. Rev. D **53**, 5799 (1996) [arXiv:hep-ph/9512263].
- [54] J. Knoll, Yu. B. Ivanov and D. N. Voskresensky, Annals Phys. **293**, 126 (2001) [arXiv:nucl-th/0102044].
- [55] M. A. York and G. D. Moore, Phys. Rev. D **79**, 054011 (2009) [arXiv:0811.0729 [hep-ph]].
- [56] P. Romatschke, Class. Quant. Grav. **27**, 025006 (2010) [arXiv:0906.4787 [hep-th]].
- [57] W. Israel, Ann. Phys. **100** (1976) 310.
- [58] W. Israel and J. M. Stewart, Annals Phys. **118**, 341 (1979).
- [59] S. A. Hartnoll, P. K. Kovtun, M. Muller and S. Sachdev, Phys. Rev. B **76**, 144502 (2007) [arXiv:0706.3215 [cond-mat.str-el]].
- [60] see for example, P. M. Morse, H. Feshbach, *Methods of theoretical physics*, New York (McGraw-Hill, 1953).
- [61] see for example, P. Roe and M. Arora, Numerical Methods for Partial Differential Equations **9**, 459 (1993).
- [62] see for example: W. H. Press *et al.*, “*Numerical Recipes 3rd Edition: The Art of Scientific Computing*”, (Cambridge University Press, 2007).